
Symmetry constraints on spin order transfer in parahydrogen-induced polarization (PHIP)

Andrey N. Pravdivtsev^{1,*}, Danila A. Barskiy^{2,*}, Jan-Bernd Hövener¹ and Igor V. Koptug³

¹ Section Biomedical Imaging, Molecular Imaging North Competence Center (MOIN CC), Department of Radiology and Neuroradiology, University Medical Center Schleswig-Holstein (UKSH), Kiel University, Am Botanischen Garten 14, 24118 Kiel, Germany

² Helmholtz-Institut Mainz, GSI Helmholtzzentrum für Schwerionenforschung, 55128 Mainz, Germany, Johannes Gutenberg Universität Mainz, 55099 Mainz, Germany

³ International Tomography Center, SB RAS, 3A Institutskaya st., 630090 Novosibirsk, Russia

* Correspondence: andrey.pravdivtsev@rad.uni-kiel.de and dbarskiy@uni-mainz.de

Abstract:

It is well known that the association of parahydrogen (pH₂) with an unsaturated molecule or a transient metalorganic complex can enhance the intensity of NMR signals; the effect is known as parahydrogen-induced polarization (PHIP). During the last decades, numerous methods were proposed for converting pH₂-derived nuclear spin order to the observable magnetization of protons or other nuclei of interest, usually ¹³C or ¹⁵N. Here, we analyze the constraints imposed by the topological symmetry of the spin systems on the amplitude of transferred polarization. In asymmetric systems, heteronuclei can be polarized to 100%. However, the amplitude drops to 75% in A₂BX systems and further to 50% in A₃B₂X systems. The latter case is of primary importance for biological applications of PHIP using sidearm hydrogenation (PHIP-SAH). If the polarization is transferred to the same type of nuclei, i.e. ¹H, symmetry constraints impose significant boundaries on the spin-order distribution. For AB, A₂B, A₃B, A₂B₂, AA'(AA') systems, the maximum average polarization for each spin is 100%, 50%, 33.3%, 25%, and 0, respectively, when A and B (or A') came from pH₂. We also discuss the effect of dipole-dipole induced pH₂ spin-order distribution in heterogeneous catalysis or nematic liquid crystals. Practical examples from the literature illustrate our theoretical analysis.

Keywords: parahydrogen; polarization transfer; symmetry constraints; PHIP, PASADENA, ALTADENA, nuclear spin isomers, symmetry groups.

1. Introduction

Parahydrogen-induced polarization (PHIP) is a cost-efficient method to polarize nuclear spins[1]. PHIP exploits the symmetry of molecular dihydrogen that exists as two nuclear spin isomers: parahydrogen (pH₂) and orthohydrogen (oH₂). The nuclear spin state of pH₂ is the singlet state, $|S\rangle = \frac{|\alpha\beta\rangle - |\beta\alpha\rangle}{\sqrt{2}}$, which is asymmetric under exchange of the nuclear spins. The total wave functions of the H₂ nuclei is antisymmetric under exchange of two nuclei (two fermions), so that the quantum numbers of the rotational states take even values [2]. oH₂ is represented by three nuclear spin states, $|T_0\rangle = \frac{|\alpha\beta\rangle + |\beta\alpha\rangle}{\sqrt{2}}$, $|T_+\rangle = |\alpha\alpha\rangle$, $|T_-\rangle = |\beta\beta\rangle$. These three states are symmetric, hence necessitating odd rotational quantum numbers[2]. This selection is dictated by the generalized Pauli principle, which states that the total wave function of two protons (two fermions with spin-1/2) is antisymmetric upon permutation.[2] Note, however that hydrogen consisting of a proton and an electron (i.e. two fermions) is a boson, hence total wave function of H₂ is symmetric under exchange of two atoms (discussed more below). The gap between the lowest two rotational energy levels, i.e. pH₂ and oH₂, is significant (170.5 K), so that 50% pH₂ can be obtained by cooling H₂ to liquid nitrogen temperatures [3] or even higher enrichment of 99% with a two-stage cryo-systems operating at 20 K [4,5].

The density matrix for an ensemble of molecules containing N spin- $1/2$ nuclei (with spins A and B originating from pH_2 molecule) can be written as follows:

$$\hat{\rho}_S^{A,B} = \frac{\hat{1}^N}{2^N} - \frac{1}{2^{N-2}} (\hat{\mathbf{I}}^A \cdot \hat{\mathbf{I}}^B). \quad (1)$$

Here, $\hat{1}^N$ is the identity matrix, i.e., a $\{2^N \times 2^N\}$ matrix with ones on the diagonal. The individual spin operators $\hat{I}_k^{A,B}$ in the dot product, $(\hat{\mathbf{I}}^A \cdot \hat{\mathbf{I}}^B) = \hat{I}_X^A \hat{I}_X^B + \hat{I}_Y^A \hat{I}_Y^B + \hat{I}_Z^A \hat{I}_Z^B$, are obtained using the Kronecker (direct) product \otimes of the corresponding Pauli matrices \hat{s}_k (with $k = X, Y$ or Z) with the 2×2 identity matrix $\hat{1}^1$. Here, the numbering of the spins in the molecule is important. For example, for the first spin, the operator is constructed as

$$\hat{I}_k^1 = \frac{1}{2} \hat{s}_k \otimes \hat{1}^1 \dots \otimes \hat{1}^1. \quad (2)$$

There are two primary variants of PHIP: (a) hydrogenative PHIP, such as PASADENA (parahydrogen and synthesis allow dramatically enhanced nuclear alignment [6]) and ALTADENA (adiabatic longitudinal transport after dissociation engenders net alignment [7]), and (b) non-hydrogenative PHIP, or SABRE (signal amplification by reversible exchange [8]), where pH_2 and substrate interact via a reversible exchange at a catalyst. Both methods have found applications at high ($\sim T$) [9], low ~ 1 mT [10], ultra-low ~ 1 μT [11,12] and zero fields [13]. To limit the scope of this paper, however, we focus our discussion on hydrogenative PHIP at high magnetic fields only. It should be noted that a similar analysis for four spin- $1/2$ SABRE system was recently performed [14].

For hydrogenative PHIP, the spin state of the molecule after pH_2 addition strongly depends on the coupling regime. Two spins $\hat{\mathbf{I}}^A$ and $\hat{\mathbf{I}}^B$ are considered strongly coupled when the difference of their Larmor precession frequencies, $\delta\nu_{AB} = |\nu_A^0 - \nu_B^0|$, is much smaller than their mutual indirect spin-spin coupling J_{AB} , i.e., $\delta\nu_{AB} \ll |J_{AB}|$. In the opposite case, the spins are weakly coupled [15]. The frequency $\nu_{A,B}^0 = \gamma_{A,B} B_0 (1 + \delta_{A,B}) / 2\pi$ of spin $\hat{\mathbf{I}}^A$ or $\hat{\mathbf{I}}^B$ depends on the strength of magnetic field B_0 , chemical shift $\delta_{A,B}$ and magnetogyric ratio $\gamma_{A,B}$.

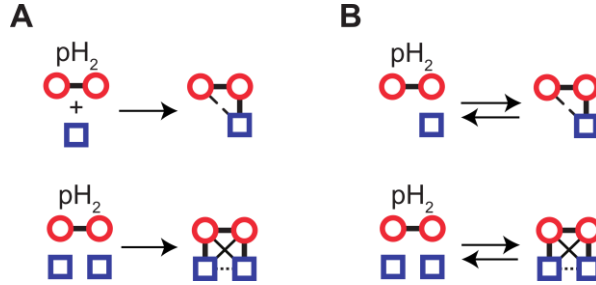


Figure 1. Schematic view of hydrogenative (A, left) and non-hydrogenative (B, right) PHIP for a 3-spin- $1/2$ system with asymmetric couplings (top) and a 4-spin- $1/2$ system with symmetric couplings (bottom). Here, we focus on hydrogenative PHIP in symmetric and asymmetric systems (A). The case of 4-spin- $1/2$ SABRE (B, bottom) was considered by Levitt in the seminal paper [14].

In the PASADENA case, upon the addition of pH_2 to an asymmetric molecular environment at high fields, ^1H spins are weakly coupled. Since individual molecular hydrogenation events are distributed in time over the course of the hydrogenation reaction, the X and Y coherences (eq (1)) are lost, and the singlet spin state $\hat{\rho}_S^{A,B}$ is averaged to the so-called ZZ spin order [1]:

$$\hat{\rho}_{ZZ}^{A,B} = \frac{\hat{1}^N}{2^N} - \frac{1}{2^{N-2}} \hat{I}_Z^A \cdot \hat{I}_Z^B. \quad (3)$$

From now on, we will omit operator "hats" for simplicity.

It is common to transfer pH_2 -derived spin alignment to proton and X -nuclear magnetization (e.g., ^{13}C , ^{15}N , ^{19}F) for use as a MR imaging contrast agent [16–18], monitoring of chemical and enzymatic reactions [19,20], or for the purpose of analytical chemistry

[21]. Many of such spin-order transformations are represented by unitary transformations of the density matrix:

$$\rho(t) = U(t, t_0)\rho(t_0)U(t, t_0)^\dagger, \quad (4)$$

where $\rho(t_0)$ is the density matrix at time t_0 , before the spin-order transfer (SOT), and $\rho(t)$ is the final density matrix, after the SOT. The unitary evolution operators $U(t, t_0)$, also known as propagators, can be found by solving the corresponding Liouville von-Neumann equation:

$$\frac{d}{dt}U(t, t_0) = -H(t)U(t, t_0) \quad (5)$$

for a time-dependent Hamiltonian $H(t)$ and the initial condition $U(t_0, t_0) = 1^N$.

In this work, we discuss the transformation of the singlet state density matrix $\hat{\rho}_S^{A,B}$ and ‘‘PASADENA’’ density matrix $\hat{\rho}_{ZZ}^{A,B}$ to observable magnetization using general properties of unitary transformations [22,23] together with restrictions imposed by molecular symmetry [14].

2. Methods

2.1. Spin operators and observables

The general SOT from the initial spin state σ_{initial} to the desired target spin state σ_{target} under the action of propagator U can be written as

$$U\sigma_{\text{initial}}U^\dagger = \sigma_{\text{final}} = \xi\sigma_{\text{target}} + \sigma_{\text{rest}} \quad (6)$$

Where σ_{final} is the final spin state, ξ is the amplitude of the target spin state σ_{target} and σ_{rest} is the difference between σ_{final} and $\xi\sigma_{\text{target}}$ that is not relevant for our considerations. We will use ρ for density matrices and σ for spin operators or traceless density matrices.

Since the propagator U is unitary, the transformation (6) implies boundaries on the parameter ξ . There is no general way to determine all possible final states σ_{final} for undefined U . However, it is possible to obtain boundary conditions for the amplitude $\xi \in [\xi_{\text{min}}, \xi_{\text{max}}]$ and a given σ_{initial} and σ_{target} in general.

We will define the spin operator of polarization of a single spin (e.g., A) as

$$\sigma_P^A = \frac{1}{2^{N-1}} I_Z^A \quad (7)$$

and the spin operator of polarization of N spins- $1/2$ as

$$\sigma_P^N = \frac{1}{2^{N-1}} \sum_{k=1}^N I_Z^k. \quad (8)$$

Now it is straightforward to calculate a polarization, P , of one spin, or the average of many spins, using corresponding spin operators (7)(8):

$$P = \frac{\text{Tr}(\rho(t) \cdot \sigma_P)}{\text{Tr}(\sigma_P \cdot \sigma_P)}. \quad (9)$$

Here, $\rho(t)$ is the density matrix of the system at the time of interest t .

In the same fashion, the amplitude ξ of the state σ_{target} for σ_{final} after SOT can be evaluated as:

$$\xi = \frac{\text{Tr}(\sigma_{\text{final}} \cdot \sigma_{\text{target}})}{\text{Tr}(\sigma_{\text{target}} \cdot \sigma_{\text{target}})}. \quad (10)$$

We will use ξ in the following to report the maximum theoretically possible polarization ($\sigma_{\text{target}} = \sigma_P$).

2.2. No symmetry constraints [22]

The boundaries for the amplitude ξ of the target state σ_{target} after SOT (eq (6)) are

$$\xi_{\text{max}} = \|\sigma_{\text{target}}\|^{-1} \cdot (\Lambda_{\text{initial}}^\dagger \cdot \Lambda_{\text{target}}^\dagger), \quad (11)$$

$$\xi_{\min} = \|\sigma_{\text{target}}\|^{-1} \cdot (\Lambda_{\text{initial}}^{\uparrow} \cdot \Lambda_{\text{target}}^{\downarrow}),$$

$$\|\sigma_{\text{target}}\| = (\Lambda_{\text{target}}^{\uparrow} \cdot \Lambda_{\text{target}}^{\downarrow}).$$

Here, Λ_{initial} and Λ_{target} are the eigenvalue vectors of the operators σ_{initial} and σ_{target} . The arrows up (\uparrow) and down (\downarrow) indicate that these eigenvalues are sorted in an ascending or descending order. In general, $\xi_{\min} \leq \xi \leq \xi_{\max}$.

These boundaries arise because we assume all transformations to be unitary, and the initial and final states are given by Hermitian operators [22].

Because σ_{initial} and σ_{target} are traceless operators, the boundary parameters often have the same absolute value: $\xi_{\max} = |\xi_{\min}|$ unless otherwise noted.

2.3. Symmetry constraints (SC) [14,22,23]

When a system has a spin symmetry (i.e., groups of equivalent spins), only the states belonging to the same irreducible representations (Γ) of this group of symmetry G can be mixed by unitary transformations [14,22,23]. In this case, the boundary conditions can be found as:

$$\xi_{\max}^{\text{SC}} = \|\sigma_{\text{target}}\|^{-1} \sum_{\Gamma} (\Lambda_{\text{initial}}^{\uparrow, \Gamma} \cdot \Lambda_{\text{target}}^{\uparrow, \Gamma}),$$

$$\xi_{\min}^{\text{SC}} = \|\sigma_{\text{target}}\|^{-1} \sum_{\Gamma} (\Lambda_{\text{initial}}^{\uparrow, \Gamma} \cdot \Lambda_{\text{target}}^{\downarrow, \Gamma}).$$
(12)

Where $\Lambda_X^{\uparrow, \Gamma}$ are vectors of eigenvalues of the operator σ_X ($X = \text{initial or target}$) that correspond to eigenvectors belonging to the same Γ and sorted in an ascending (\uparrow) or descending (\downarrow) order.

The transformation amplitude ξ is bounded as $\xi_{\min} \leq \xi_{\min}^{\text{SC}} \leq \xi \leq \xi_{\max}^{\text{SC}} \leq \xi_{\max}$.

2.4. Eigenvalues in the case of SC

It is not trivial to define $\Lambda_X^{\uparrow, \Gamma}$ if SCs are present. To find the transformation of a density matrix σ into a *group-symmetrized* basis, one needs to construct a symmetry group specific matrix Q from orthonormal basis vectors \vec{v} . Each vector \vec{v} must belong only to one irreducible representations Γ . Vectors \vec{v} are written vertically. Let us enumerate these vectors in such a way that all vectors from the same Γ stand next to each other: $Q = (\vec{v}_1^{\Gamma_1}, \vec{v}_2^{\Gamma_1}, \vec{v}_3^{\Gamma_1}, \dots, \vec{v}_1^{\Gamma_2}, \dots, \vec{v}_m^{\Gamma_k})$. Then, the matrix of spin state σ (σ_{initial} or σ_{target}) in the new basis σ^Q can be found as

$$\sigma^Q = Q^{-1} \sigma Q. \quad (13)$$

There are three different situations for σ^Q :

1. **σ^Q is diagonal.** When the predefined basis of the group G coincides with the eigenstates of the operator σ , then σ^Q is diagonal with eigenvalues on the diagonal. All coherences (off-diagonal elements) are zero. To find $\Lambda^{\uparrow, \Gamma}$ one has only to sort and enumerate the eigenvalues inside each Γ :

$$\sigma^Q = Q^{-1} \sigma Q = \begin{pmatrix} \Lambda_1^{\Gamma_1} & 0 & \dots & 0 \\ 0 & \Lambda_2^{\Gamma_1} & & 0 \\ \vdots & \vdots & \ddots & \vdots \\ 0 & 0 & \dots & \Lambda_m^{\Gamma_k} \end{pmatrix}. \quad (14)$$

Here, $\Lambda_m^{\Gamma_n}$ is an eigenvalue of σ and $\vec{v}_m^{\Gamma_n}$ its corresponding eigenvector belonging to irreducible representations Γ_n .

2. **σ^Q is Γ -block diagonal.** When σ^Q has coherences only inside the same irreducible representations Γ , then σ^Q is Γ -block diagonal matrix

$$\sigma^Q = Q^{-1}\sigma Q = \begin{pmatrix} \Lambda^{\Gamma_1} & 0 & \cdots & 0 \\ 0 & \Lambda^{\Gamma_2} & & 0 \\ \vdots & & \ddots & \vdots \\ 0 & 0 & \cdots & \Lambda^{\Gamma_k} \end{pmatrix}. \quad (15)$$

Here, Λ^{Γ_m} are the corresponding blocks of irreducible representations Γ_m . Because all vectors from one Γ have the same symmetry, their superposition also has the same symmetry. It means that each block Λ^{Γ_m} should be additionally diagonalized, and resulting diagonal elements are corresponding eigenvalues $\Lambda_m^{\Gamma_n}$.

3. **σ^Q is not block diagonal.** The most general case is when there are off-diagonal elements between different irreducible representations.

$$\sigma^Q = Q^{-1}\sigma Q = \begin{pmatrix} \Lambda^{\Gamma_1} & C_{\Gamma_1}^{\Gamma_2} & \cdots & C_{\Gamma_1}^{\Gamma_k} \\ C_{\Gamma_2}^{\Gamma_1} & \Lambda^{\Gamma_2} & & C_{\Gamma_2}^{\Gamma_k} \\ \vdots & & \ddots & \vdots \\ C_{\Gamma_k}^{\Gamma_1} & C_{\Gamma_k}^{\Gamma_2} & \cdots & \Lambda^{\Gamma_k} \end{pmatrix}. \quad (16)$$

In this situation, we will assume that the coherences $C_{\Gamma_n}^{\Gamma_m}$ are averaged to zero during the hydrogenation reaction due to magnetic field inhomogeneity and the different evolution time of each hydrogenated molecule. When such off-diagonal elements are removed ($C_{\Gamma_n}^{\Gamma_m} := 0$), the σ^Q is " Γ -block diagonal" and equivalent to eq (15). Hence, the consequent diagonalization and analysis is equivalent and described in "case 2".

In the following discussion, we use these three methods to find eigenvalues to evaluate ξ . A script is available in SI to evaluate ξ for a different number of spins, symmetry, initial and target spin states (Matlab).

Below we will discuss some specific cases and demonstrate the effect of symmetry on PHIP and spin order transfer.

2.5. Spin systems notations

We use a notation that is slightly different from Pople's spin-system notation. The main idea is to distinguish the symmetries of the spin system. In addition, we fix X-spin to the target ^{13}C nucleus. Let us consider some examples.

First, for us, "ABC" stands for a system with three chemically nonequivalent spins and only weak coupling is considered between spins. Second, according to Pople's notation, $^{12}\text{C}_2$ -ethylene consists of four chemically and magnetically equivalent ^1H spins, hence the spin symmetry is A_4 . However, it does not reflect the permutation group symmetry of ethylene. Hence, we refer to spin symmetry of $^{12}\text{C}_2$ -ethylene as $AA'(AA')$.

3. Results

Note that the polarizations reported in the following are the upper limit of what can be transferred theoretically (as implied by the transformation mathematics).

3.1. Parahydrogen spin-order transfer in a two spin- $1/2$ system

3.1.1. The symmetry of AB and A_2 systems

The simplest PHIP system consists of two spin- $1/2$ nuclei. If the protons of pH_2 after hydrogenation are magnetically and chemically nonequivalent (AB-system) – no symmetry constrains. The spins can be treated separately and the appropriate basis would be the *Zeeman* basis:

$$S^{AB} = \{|\alpha\alpha\rangle, |\alpha\beta\rangle, |\beta\alpha\rangle, |\beta\beta\rangle\}. \quad (17)$$

When the protons are magnetically equivalent, the system is called A_2 that imposes restrictions on the choice of the basis. Here singlet-triplet (S-T) states should be used:

$$S^{A_2} = \{|S\rangle, |T_+\rangle, |T_0\rangle, |T_-\rangle\}. \quad (18)$$

Among these two systems, only A_2 has nontrivial symmetry, which is C_2 . In **Appendix A** we describe all relevant groups of symmetry. The transformation elements of C_2 group are identity transformation E or null permutation "()" and permutation of two protons $\begin{pmatrix} 12 \\ 21 \end{pmatrix} = (21)$:

$$G^{12} = \{(), (21)\}. \quad (19)$$

The C_2 group (or G^{12}) has two irreducible representations: even (gerade - "g") and odd (ungerade - "u"). The singlet state is the only member of odd irreducible representation $\Gamma^u=B$, while three triplet states are the members of $\Gamma^g=A$. In terms of sets, it can be written as

$$\begin{aligned} S_A^{12} &= \{|T_+\rangle, |T_0\rangle, |T_-\rangle\}, \\ S_B^{12} &= \{|S\rangle\}. \end{aligned} \quad (20)$$

Tables of characters and decomposition of spin states into irreducible representations are given for A_2 , A_3 , AA' (AA') systems in **Appendix A**.

3.1.2. pH₂ to magnetization in AB systems

Let us consider the transformation of $\sigma_{ZZ}^{A,B}$ spin order in an AB system (no symmetry constraints, eq (11)) to magnetization (eq (7)(8)):

$$\sigma_{ZZ}^{A,B} = -I_Z^A \cdot I_Z^B \rightarrow \begin{cases} \frac{1}{2} I_Z^{A, \text{or } B}, & |\xi| = 1, \\ \frac{1}{2} [I_Z^A + I_Z^B], & |\xi| = \frac{1}{2}, \\ \frac{1}{2} [I_Z^A - I_Z^B], & |\xi| = \frac{1}{2}. \end{cases} \quad (21)$$

This means that PASADENA spin order ($\sigma_{ZZ}^{A,B}$) can be transferred to 100% polarization of one spin, or 50% polarization of each spin. In the latter case, the net magnetization can be 50% per spin or zero (21).

The examples of spin-order transfer (SOT) sequences for direct polarization transfer to one spin are Selective Excitation of Polarization using PASADENA (SEPP)[24] and adiabatic-passage spin order conversion (APSOC)[25–27]. SOT for polarization transfer to two spins include out of phase echo (OPE)[28], only parahydrogen spectroscopy (OPSY)[28,29] and APSOC[25–27].

3.1.3. pH₂ to magnetization in A₂ systems

The situation is different for two magnetically equivalent spins A^1 and A^2 in an A_2 spin system. Symmetry constraints do not allow spin order conversion of $\sigma_S^{A,B}$ into net magnetization:

$$\sigma_S^{A^1, A^2} = -(\mathbf{I}^{A^1} \cdot \mathbf{I}^{A^2}) \rightarrow \frac{1}{2} I_Z^{A^1} + \frac{1}{2} I_Z^{A^2}, \quad |\xi^{SC}| = 0 \quad (22)$$

The only way to transfer polarization is to break the symmetry ($A_2 \rightarrow AB$) that is happening e.g. during ALTADENA.

3.1.4. Limitation of the method: ALTADENA example

One of the first experiments that demonstrated spin order conversion of pH₂ was ALTADENA [7], using adiabatic magnetic field variation (AMFV). AMFV-induced spin order transfer in an AB, two spin- $\frac{1}{2}$ system results in the following transformation of $\sigma_S^{A,B}$ [1]:

$$\sigma_S^{A,B} = -(\mathbf{I}^A \cdot \mathbf{I}^B) \xrightarrow{\text{AMFV}} -I_Z^A \cdot I_Z^B \pm \frac{1}{2}(I_Z^A - I_Z^B). \quad (23)$$

The sign (\pm) depends on the relative chemical shift difference and the sign of J -coupling constant of the spins [1]. It follows that in ALTADENA, both spins acquire maximum polarization of 1 (see eq (7)), but the total (net) polarization of the molecule is zero.

The Hamiltonian of an AB system H_{AB} is, in general, asymmetric (lacking permutation symmetry). However, at zero field ($B_0 = 0$), it has the same permutation symmetry as the Hamiltonian of A_2 system H_{A_2} :

$$\begin{aligned} H_{AB}(B_0 \neq 0) &= -v_A^0 I_Z^A - v_B^0 I_Z^B + J_{AB}(\mathbf{I}^A \cdot \mathbf{I}^B), \\ H_{AB}(B_0 = 0) &= J_{AB}(\mathbf{I}^A \cdot \mathbf{I}^B), \end{aligned} \quad (24)$$

$$H_{A_2}(B_0 \neq 0) = -v_A^0(I_Z^1 + I_Z^2) + J_{A^1 A^2}(\mathbf{I}^{A^1} \cdot \mathbf{I}^{A^2}).$$

This means that the initial and final symmetries of the Hamiltonian (and the spin system) are different and eq (12) cannot be used for the estimation of ξ^{SC} (i.e., the symmetry changes during the experiment). We do not introduce a calculation method for such situations.

However, notice that the symmetry of the Hamiltonian (24) changes by introducing a magnetic field, while molecular symmetry does not change. This means that molecular symmetry does not have to coincide with the spin symmetry (or the symmetry of the nuclear spin Hamiltonian). The latter is essential for SOT, but molecular symmetry is essential for spin isomers (discussed below). Thus, there are at least three relevant symmetries: the Hamiltonian, interactions, and the spatial configuration of the molecule.

3.1.5. pH₂ on the a surface of a solid

It was predicted that the spin order of pH₂ after chemisorption, i.e. interaction with a surface, could be transformed into net magnetization even when the two spins have the same chemical shifts [30,31]. Note that there are a minimum of two requirements for PHIP via chemisorption: (a) the pH₂ nascent protons have to be chemically nonequivalent, and (b) if they split, there is a non-zero chance to reunite again with preserved quantum coherences. The main reason for spin order conversion is the difference in chemical shifts and intramolecular dipole-dipole (DD) interaction which is relevant on the surface. The Hamiltonian of such AB system at zero-field is

$$H_{AB}^{DD}(B_0 = 0) = J_{AB}(\mathbf{I}^A \cdot \mathbf{I}^B) + d(\theta, \varphi) \left(3I_Z^A \cdot I_Z^B - (\mathbf{I}^A \cdot \mathbf{I}^B) \right). \quad (25)$$

As a result, the state of the dihydrogens after chemisorption of pH₂ is expected to be a superposition of $\sigma_S^{A,B}$ and $\sigma_{ZZ}^{A,B}$ [31]:

$$\sigma_{S-DD}^{A,B} = -(P_{ZZ} - P_S)I_Z^A \cdot I_Z^B - P_S(\mathbf{I}^A \cdot \mathbf{I}^B). \quad (26)$$

Where P are the relative weights of the states σ_S and σ_{ZZ} . This result was predicted for two AB spins with the Hamiltonian H_{AB}^{DD} (eq (26)) by averaging the pH₂ derived initial spin state, $\sigma_S^{A,B}$, over hydrogenation time period.

We showed before that it is impossible to transfer $\sigma_S^{A,B}$ to total net magnetization of two spins in an A_2 system (eq (22)). However, it is possible to transfer $\sigma_{ZZ}^{A,B}$:

$$\sigma_{ZZ}^{A,B} = -I_Z^A \cdot I_Z^B \rightarrow \frac{1}{2}[I_Z^A + I_Z^B], \quad |\xi^{SC}| = 0.5, \quad (27)$$

even with symmetry constraints. Note that $|\xi^{SC}| = |\xi| = 0.5$ (compare eq (21) and eq (26)).

However, one should bear in mind that the mere feasibility of such transfer computed using the presented approach does not take into account whether or not there are interactions in the system that can be used for observation of the resulting spin order. Using solid echo sequences, SOT from $\sigma_{ZZ}^{A,B}$ to $\sigma_P^{A,B}$ was predicted for chemisorbed pH₂ [32,33].

3.2. Transfer of pH₂ spin order to ¹H magnetization in multispin systems

3.2.1. No symmetry constraints

Now we will consider the transfer of either $\sigma_{ZZ}^{A,B}$ or $\sigma_S^{A,B}$ spin order into total spin magnetization, σ_P^N (eq (8)), in N spin-1/2 systems with various topologies (**Figure 2**).

The highest level of polarization (i.e., the average polarization across all coupled spins) is possible if the system is in a pure singlet state $\sigma_S^{A,B}$ rather than in $\sigma_{ZZ}^{A,B}$ (**Figure 3 and 4 and Appendix B, tables B1, B2**).

This situation is achieved when the S-T states are a (stationary) eigenbasis, i.e. when the J-couplings dominate the interactions. This can be achieved by adding pH₂ at low fields like in ALTADENA or via strong RF-pulses suppressing chemical shift evolution at high field [34]. Spin order transfer at low field can be realized using SLIC pulses and was demonstrated for molecular systems with up to five nonequivalent spins [35].

Interestingly, the maximum achievable polarization per molecule increases up to 400% (i.e. the equivalent of 4 spins polarized to 100%) if the system has 9 spins or more and the initial density matrix is $\sigma_S^{A,B}$.

3.2.2. With symmetry constraints

When a spin system has any permutation symmetries, the theoretically achievable proton polarization drops significantly. For example, in the A₃B₂C system of ethanol, the maximum average polarization is only 14.2% if pH₂ were added pairwise in positions A and B. If the symmetry constraints are relaxed so that six spins nonequivalent result, the maximum achievable polarization increases to 31.2% for $\sigma_{\text{initial}} = \sigma_{ZZ}^{A,B}$ and 50% for $\sigma_{\text{initial}} = \sigma_S^{A,B}$, respectively (**Figure 3**).

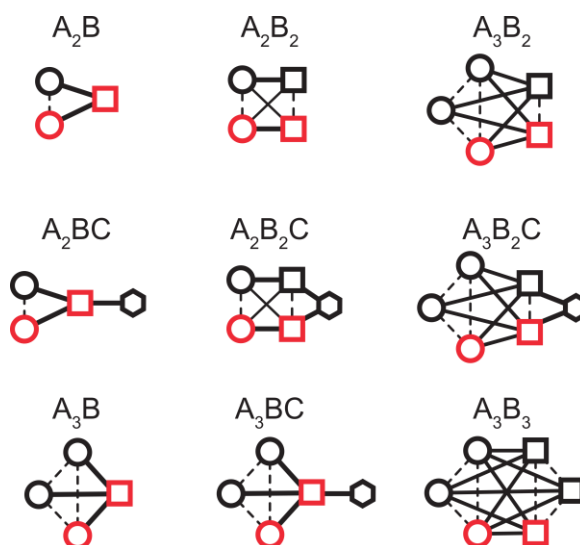


Figure 2. Spin topologies considered for simulating the effect of symmetry on the transformation of pH₂-derived spin order (red) into observable polarization. Red symbols indicate the pH₂-nascent spins, different lines indicate J-coupling constants, circles, squares, hexagons are spins of the same type.

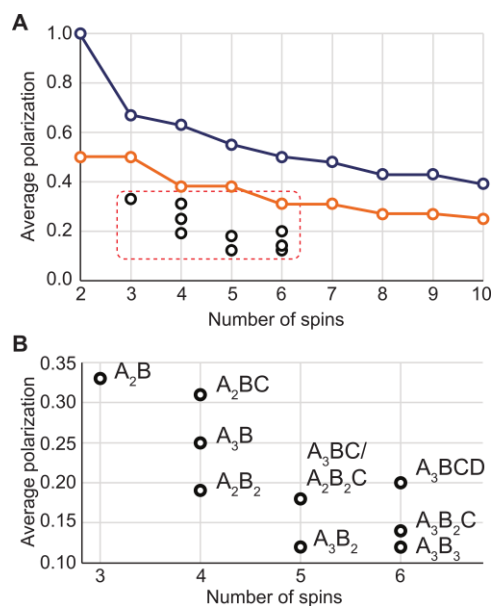


Figure 3. Average polarization per spin that can be achieved theoretically by adding pHz to a molecule with 2 – 10 spins with (black) and without (orange, blue) symmetry constraints. In general, higher polarization can be achieved if there are no constraints (compare black with orange and blue) and if the initial density matrix is $\sigma_S^{A,B}$ (blue) rather than $\sigma_{ZZ}^{A,B}$ (orange, compare blue and orange in A). We assumed pHz to be added in positions A and B. The reported values are given in **tables B1 and B2 (Appendix B)**.

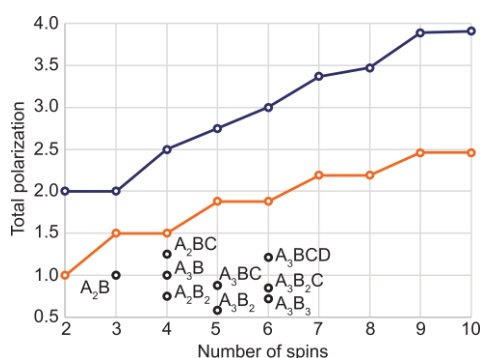


Figure 4. Sum of the average polarization – in units of one-spin polarization – that can be achieved theoretically by adding pHz to a molecule with 2 – 10 spins with (black, $\sigma_S^{A,B} \rightarrow \sigma_P^N$) and without symmetry constraints for $\sigma_S^{A,B} \rightarrow \sigma_P^N$ (blue) and $\sigma_{ZZ}^{A,B} \rightarrow \sigma_P^N$ (orange). If the polarization of all spins are summed up, up to ~ 400 % and above for more spins was obtained for large spin systems (blue). The reported values can be obtained from the average values given in **tables B1, B2 (Appendix B)**.

3.2.1. Nuclear spin isomers of H₂ and ethylene

Dihydrogen. We introduce nuclear spin isomers of molecules (NSIM), starting with H₂. The molecular symmetry group of H₂ is $D_{\infty h}$, while the permutation symmetry group of two spins is only C₂. The $D_{\infty h}$ symmetry include an infinite number of symmetry elements and is a product of C₂ and C_∞ rotation groups, S_∞ rotation-reflection and C_v groups. For the sake of simplicity, and to exemplify NSIM, let us consider the C₂ symmetry only. The four nuclear spin states (sp) of H₂ can be grouped in two sets A and B (eq (20) and **Appendix A**): A^{sp} (3 states, oH₂) and B^{sp} (1 state, pHz).

Ethylene. Ethylene is another example of a molecule with different NSIMs. Unlike H₂, however, the molecular symmetry group of ethylene is D_{2h}. Although the permutation symmetry group of spins is D₂ [36], it is helpful to use molecular symmetry to have a connection to corresponding rotational symmetries.

The permutation D_2 subgroup consists of 1 trivial and three nontrivial permutations that correspond to three orthogonal 180° rotations (**Figure 5**). In the D_2 symmetry group (see **Appendix A**), the 16 spin (sp) states of ethylene are grouped in 4 sets that correspond to A^{sp} , B_1^{sp} , B_2^{sp} and B_3^{sp} symmetries; seven states for A-symmetry set and 3 states for each of B-symmetry sets.

D_{2h} symmetry group includes additional inversion operation (**i**) and its combinations with the above-mentioned 180° rotations. In this case, the decomposition of 16 spin states also results in 4 groups with additional symmetry indices: A_g^{sp} (7 states), B_{1u}^{sp} (3 states), B_{2u}^{sp} (3 states) and B_{3g}^{sp} (3 states). Seven states of A_g^{sp} symmetry include five states with total spin 2 ($A_{g,2}^{sp}$) and two states with total spin 0 ($A_{g,0_1}^{sp}$ and $A_{g,0_2}^{sp}$). Each B group corresponds to three spin states of the same symmetry with the total spin 1.

The parity of spin states is even, and so is the parity of these four groups of symmetry. The rotational wavefunctions of ethylene are all of g symmetry, which leaves only four rotational (rot) symmetries A_g^{rot} , B_{1g}^{rot} , B_{2g}^{rot} , B_{3g}^{rot} .

The total (rotational and nuclear spin) wavefunction should have A-symmetry (either A_g or A_u), therefore there are again four allowed combinations for ethylene: $A_g^{rot}A_g^{sp}$, $B_{1g}^{rot}B_{1u}^{sp}$, $B_{2g}^{rot}B_{2u}^{sp}$, $B_{3g}^{rot}B_{3g}^{sp}$.

We discuss the ethylene case in detail because it gives very good insights for the problem of polarization transfer between states of different symmetries.

Upon NSIM interconversion, the associated energy changes are by far larger than what is normally induced in NMR by RF pulses. A NSIM interconversion inevitably changes both rotational and spin states of ethylene. This is in strong contrast to non-symmetric molecules where the energy of spin flips is comparable to the strength of nuclear spin interactions. The large gap between H_2 rotational energies helps to enrich p H_2 state at low temperatures and is responsible for its long lifetime [3,5].

It may happen that some of the states belonging to different NSIM of polyatomic molecules have similar energies (in contrast to H_2 for which this is impossible). Such gateways are the basis of the quantum relaxation theory of NSIM interconversion [37]. For instance [38], for the $B_{1g}^{rot}(J=23)B_{1u}^{sp}$ and $B_{2g}^{rot}(J=21)B_{1g}^{sp}$ states of ethylene, the energy gap is "only" 46 MHz, i.e., within the reach of dipolar couplings. However, the energy of these states is 900 cm^{-1} (1300 K) above the ground state of ethylene; therefore, their thermal population is low and the NSIM interconversion is also relatively slow despite efficient mixing of these states by the dipole-dipole interaction.

Unlike in H_2 (with C_2 symmetry), in ethylene, it seems possible to transfer singlet state and ZZ spin order into magnetization:

$$\begin{aligned}\sigma_S^{Am,An} &= -\frac{1}{4} \mathbf{I}^{Am} \cdot \mathbf{I}^{An} \rightarrow \frac{1}{8} (I_Z^{A1} + I_Z^{A2} + I_Z^{A3} + I_Z^{A4}) \\ \sigma_{ZZ}^{Am,An} &= -\frac{1}{4} I_Z^{Am} \cdot I_Z^{An} \rightarrow \frac{1}{8} (I_Z^{A1} + I_Z^{A2} + I_Z^{A3} + I_Z^{A4})\end{aligned}\quad (28)$$

with Am and An being one of four protons. Using the ethylene J -coupling constants to set the basis of spin states (**Appendix A** and ref [19], $J_g=1.07\text{ Hz}$, $J_c=11.47\text{ Hz}$ and $J_t=17.78\text{ Hz}$ [39]), the following values were obtained for different hydrogenation sites: $|\xi_{S,cis}^{SC}| = |\xi_{S,trans}^{SC}| = |\xi_{S,gem}^{SC}| = 0.2$ and $|\xi_{ZZ,cis}^{SC}| = |\xi_{ZZ,trans}^{SC}| = |\xi_{ZZ,gem}^{SC}| = 0.225$. According to **Figure 5**, here cis corresponds to protons 1 and 4 (or 2 and 3), trans to 1 and 3 (or 2 and 4), gem to 1 and 2 (or 3 and 4). Note that using other simulations or isotop-labelling other (but similar) values were obtained and can be used [40]: $J_g=2.23 - 2.39\text{ Hz}$, $J_c=11.62 - 11.66\text{ Hz}$ and $J_t=18.99 - 19.03\text{ Hz}$; [41]: $J_g=2.5\text{ Hz}$, $J_c=11.6\text{ Hz}$ and $J_t=19.1\text{ Hz}$. However, because the constants of the same order we did not compare the spin order transfer for different J -coupling values.

It may come as a surprise that efficient transfer of singlet spin order to polarization is feasible in a highly symmetric system like ethylene. So far, this transfer was demonstrated only in aligned media (nematic liquid crystals), where dipole-dipole spin-spin interactions

remain, and the Hamiltonian of the system resembles H_{AB}^{DD} (eq (25)). For such Hamiltonian as discussed above, instead of pure $\sigma_S^{Am,An}$, a mixture of $\sigma_S^{Am,An}$ and $\sigma_{ZZ}^{Am,An}$ should be considered and $\sigma_{ZZ}^{Am,An}$ spin order is observable in NMR.

Normally, the transition between two states with spin 0 that are represented by $A_{g,0_1 \text{ or } 2}^{sp}$ and $A_{g,2}^{sp}$ symmetries can not be observed by NMR. However, the theory applied here still allows the transfer of spin order to polarization. Let's have a closer look and find out why this is possible.

After hydrogenation with pH_2 , six states with B-symmetry and two singlets of A_g symmetry are populated under each hydrogenation scenario (**Table 1**). The average polarization that we considered in eq (28) depends on the populations of all symmetry states and is not straightforward to analyze. But let us instead consider the state $|2,2\rangle = |\alpha\alpha\alpha\alpha\rangle$ with the maximum for the system value of spin and spin projection of 2; one of five states of A_g^{sp} symmetry. It means that if there is a way to transfer polarization from one of two $|0,0\rangle$ spin states ($A_{g,0_1 \text{ or } 2}^{sp}$) to the $|2,2\rangle$ state (both have the same A_g^{sp} symmetry), ethylene hyperpolarization will be revealed. Now the question remains, how to achieve this, and if any existing spin order transfer methods, e.g. spin-lock induced crossing (SLIC)[42], adiabatic passage spin order conversion (APSOC)[27] or magnetic field cycling (MFC)[43] are suitable. This analysis goes beyond the scope of this paper and will be considered elsewhere.

Table 1. Relative populations of spin symmetries in ethylene after addition of pH_2 in germinal (gem), cis and trans position. Note that there are also coherences between $A_{g,0_1}^{sp}$ and $A_{g,0_2}^{sp}$ states, and between the two respectively populated B-symmetries (e.g. B_{2u}^{sp} and B_{3g}^{sp} in case of pos. = gem).

Pos.	$A_{g,2}^{sp}$	$A_{g,0_1}^{sp}$	$A_{g,0_2}^{sp}$	B_{1u}^{sp}	B_{2u}^{sp}	B_{3g}^{sp}
gem	0	0.2409	0.009	0	1/8	1/8
cis	0	0.1075	0.1425	1/8	0	1/8
trans	0	0.0266	0.2234	1/8	1/8	0

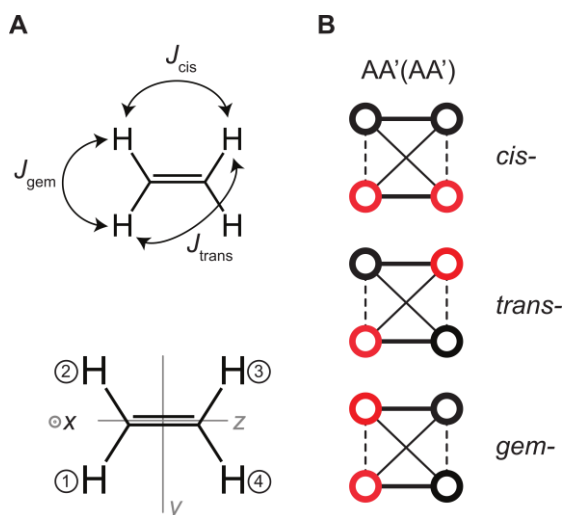


Figure 5. Interactions and symmetry axis of ethylene . A) Drawing of ethylene and its nuclear spin-spin couplings (J -couplings, top), numbering of the atomic positions and the cartesian axis x, y, z . B) Graphs corresponding to the spin system $AA'(AA')$ where pH_2 was added at cis-, trans- or geminal positions (red circles). Different lines corresponds to different values of spin-spin interactions.

3.3. PHIP-SAH and the transfer of pH_2 spin order to the magnetization of X-nuclei

3.3.1. PHIP-SAH

Polarization transfer from pH_2 to X-nuclei also attracts significant attention in the context of hyperpolarized MRI applications. The lack of background signal and extended

lifetime of polarization (compared to ^1H) makes hyperpolarized MRI of X-nuclei highly interesting for biomedical applications, spearheaded by hyperpolarized MRI of xenon and ^{13}C -pyruvate. [16,44–47]

PHIP by sidearm hydrogenation (PHIP-SAH)[48,49] (**Figure 6**) attracted significant attention because it allowed polarization of acetate and pyruvate – the most commonly used contrast agents for hyperpolarized in vivo MRI. [50,51]

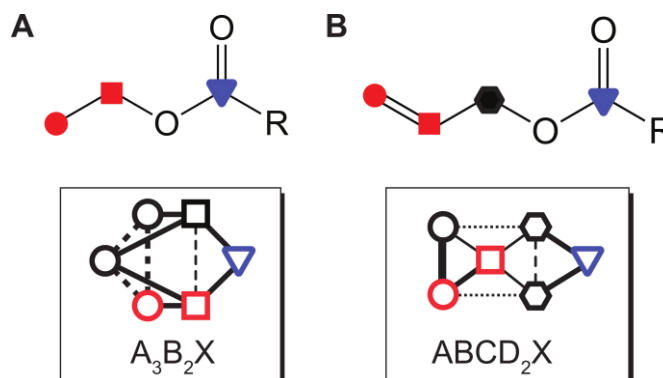


Figure 6. Molecular structures (top) and spin topologies (bottom) of ethyl (A) and allyl (B) esters: of carboxylic acids - products of PHIP-SAH. Different lines (bottom) represent different spin-spin interaction values.

3.3.2. No symmetry constraints

We considered the transfer of $\sigma_S^{A,B}$ (1) and $\sigma_{ZZ}^{A,B}$ (3) to X-nuclear polarization (σ_P^X) (7) without symmetry constraints (**Table 2**). In both cases, 100% polarization can be achieved: $|\xi| = 1$. This, for example, was predicted for hydrogenation of perdeuterated 1- ^{13}C -vinyl-acetate- d_6 [9]. More than 50% polarization was achieved on ^{13}C in the system consisting of three nonequivalent spin- $1/2$ and six spin-1 nuclei (^2H). The direct loss of polarization is due to S- T_0 mixing of p H_2 -derived hydrogens at the catalyst and relaxation during hydrogenation [52].

3.3.3. Symmetry constraints

If some other (i.e., non nascent p H_2) protons possess any symmetry, still, 100% polarization transfer can be achieved on X (theoretically). This situation is realized e.g. in 1- ^{13}C -allyl-pyruvate, an ABCD $_2$ X system.

If one of the p H_2 -nascent protons ends up in a symmetric site of the product, the maximum polarization that can be transferred to X is reduced to 75% for A $_2$ BX ($|\xi^{\text{SC}}| = 3/4$) and 66.(6)% for A $_3$ BX ($|\xi^{\text{SC}}| = 2/3$). Again, the number of the "other" protons and their symmetry does not play a role.

If both p H_2 spins bind to two different symmetric spin sites, like A $_3$ B $_2$ X, A $_3$ B $_2$ C $_2$ X, the maximum polarization that can be transferred to X is further reduced to 50% ($|\xi^{\text{SC}}| = 0.5$). This situation is found in ethyl- and propyl pyruvate e.g.

In the literature, about 20% ^{13}C -polarization was reported on ethyl pyruvate. Here, p H_2 was added to vinyl pyruvate at high field and spin order was transferred to ^{13}C using INEPT [53]. About 20-35% ^{13}C -polarization was reported in a similar experiment, where p H_2 was added at low field and after magnetic field variation detection took place at high field [43,54]. However, one should remember that, as with the ALTADENA case discussed above, the Hamiltonian of the system changes during the magnetic field variation.

It is interesting to note that it is not possible to transfer spin order in an A $_3$ X system if two of the A spins are in the singlet state ($|\xi^{\text{SC}}| = 0$ for $\sigma_S^{A_i A_j} \rightarrow \sigma_P^X$). If they are in the "reduced" singlet state σ_{ZZ} , however, transfer is possible ($|\xi^{\text{SC}}| = 1/3$ for $\sigma_{ZZ}^{A_i A_j} \rightarrow \sigma_P^X$). For example, as we discussed before, p H_2 derived spin order after chemisorption is partially in ZZ state.

Table 2. Polarization transfer from pHz ($\sigma_S^{A,B}$) to an X nucleus (σ_P^X). One hydrogen of pHz is in A, the other is in B position.

Type of the system	ξ_{\max} from $\sigma_S^{A,B} = \xi\sigma_P^X + \sigma_{\text{rest}}$	Examples of molecule, R=acetate, pyruvate
ABX, ABCX, ABCDX, ABCDEX,...	1	1- ¹³ C-vinyl-R
ABCD ₂ X		1- ¹³ C-allyl-R
AA'BB'X	1	1- ¹³ C-ethylene
A ₂ BX	3/4	
A ₂ BC ₂ X	3/4	
A ₃ BX	2/3	
A ₂ B ₂ X	9/16	
A ₃ B ₂ X	1/2	1- ¹³ C-ethyl-R
A ₃ B ₂ C ₂ X	1/2	1- ¹³ C-propyl-R

3.3.4. Double hydrogenation

Now we turn to the question: is it beneficial to add two pHz molecules to one target? For example, 1-¹³C-ethynyl pyruvate is transformed into 1-¹³C-ethyl pyruvate, an A₃B₂X system, by double hydrogenation (addition of two pHzs). Likewise, 1-¹³C-propargyl pyruvate becomes 1-¹³C propyl pyruvate, an A₃B₂C₂X system, upon addition of two pHz (pHz is added to A and B in both cases).

Let us assume that the hydrogenation reaction is so fast that only the $|SS\rangle\langle SS|$ spin state is populated, which can be written as

$$\sigma_{S|S}^{A1,B1|A2,B2} = -\frac{1}{2^{N-2}} (\mathbf{I}^{A1} \cdot \mathbf{I}^{B1}) - \frac{1}{2^{N-2}} (\mathbf{I}^{A2} \cdot \mathbf{I}^{B2}) + \frac{1}{2^{N-4}} (\mathbf{I}^{A1} \cdot \mathbf{I}^{B1})(\mathbf{I}^{A2} \cdot \mathbf{I}^{B2}) \quad (29)$$

The theoretically maximum transfer from $\sigma_{S|S}^{A1,B1|A2,B2}$ to X-nuclear polarization in A₃B₂X and A₃B₂C₂X systems is $|\xi^{SC}| = 1/4$: 2 times lower than for the single hydrogenation. Note that it is also system specific, e.g. for A₂B₂X system double hydrogenation results in $|\xi^{SC}| = 3/4$, while $|\xi^{SC}| = 9/16$ is a maximum predicted for a single hydrogenation (Tab. 2).

In reality, however, there will be a finite time between the first and second hydrogenation, such that the system will start to evolve. As a result, the final state will be different than $|SS\rangle\langle SS|$ and the polarization of X nucleus will also be different.

The situation is similar for multiple hydrogenations in different positions as, for example, in trivinyl orthoacetate.[55] If we simplify the product to two ethyl groups, the system becomes (A₃B₂)(A₃B₂)'X, where one pHz is part of the A₃B₂ subsystem, and the other is part of (A₃B₂)' subsystem. In this case, polarization transfer amplitude $|\xi^{SC}| = 5/16$ was predicted, while for a single hydrogenation (yielding an A₃B₂X system), it was $|\xi^{SC}| = 1/2$.

3.4. Examples of isotopic and chemical symmetry breaking

3.4.1. Ethylene

Ethylene produced by adding pHz to acetylene in isotropic environment does not demonstrate any enhanced observable magnetization. The spin state of pHz should be converted into ZZ-state instead: this was demonstrated after hydrogenation and subsequent dissolution of ethylene in a liquid crystal [19]. However, one can imagine to do it in different

order. First, generate the ZZ-state of pH₂ derived H₂, that was estimated for solid catalyst [30,31]. Second, hydrogenate acetylene using this H₂.

In genera, the pH₂-derived protons are observed only when they are attached to chemically or magnetically inequivalent sites that for ethylene can be achieved at least in two ways:

- The two pairs of hydrogens in ethylene can be made magnetically nonequivalent by ¹³C labeling. In case of single-sided ¹³C labeling system symmetry drops down to C₂ and polarization transfer is possible to ¹H or ¹³C nuclei. In addition, chemical shifts of two gem pairs of protons are different.
- The other way to break the ethylene symmetry is a chemical reaction. So, polarized ethylene gas bubbled through a CCl₄ solution of perfluoro(para-tolylsulfenyl) chloride (PTSC) yields an asymmetric PTSC/ethylene adduct [19]. As a result, a normal PASADENA spectrum can be obtained.

3.4.2. Fumarate and maleate

Fumarate and maleate are two metabolites with symmetry imposed spin order transfer restrictions; the solutions are also the same. The symmetry can be broken by a ¹³C labeling [56,57] or as a result of chemical reaction: "hyperpolarized" fumarate was converted by fumarase to asymmetric malate revealing itself in PASADENA spectrum [58].

Dimethyl ether of maleate (and fumarate, other popular PHIP molecule) has C_s symmetry. However, pH₂-derived protons are magnetically inequivalent because of interaction with two CH₃ groups and spin order of pH₂ can be accessed with RF pulses [56] or magnetic field variation [59].

4. Discussion

We considered several cases of polarization transfer from pH₂ to proton and X nuclei magnetization using the methods introduced in Refs. [14,22,23]. The approach used here helps to provide some general answers to several nonintuitive questions. However, a few situations remain unclear and may indicate some limitations of the presented theory. Namely,

Q1. How to estimate maximum polarization transfer from a state which is not diagonal in the basis of the system's symmetry?

Q2. How to estimate polarization transfer in systems that experience symmetry change during the polarization transfer, e.g. A₂→AB during magnetic field variation in ALTADENA experiment? Is there a general solution for an N-spin system?

Discussion of Q1. This situation corresponds to the third case of a σ^Q -diagonalization (eq (16)) as described in *methods*. For example, in an A₂BX system, the basis consists of the functions $|Mkl\rangle$ where $|M\rangle$ is one of S-T basis functions and $|k\rangle$, $|l\rangle$ are spin up and down, $|\alpha\rangle$ and $|\beta\rangle$. In this basis, $\sigma_S^{A1,B}$ is not diagonal. Instead, projecting this state on the symmetry basis results in $\frac{1}{2}[\sigma_{ZZ}^{A1,B} + \sigma_{ZZ}^{A2,B}]$, meaning that we lose part of the initial spin order and potentially underestimate the level of polarization transfer.

Discussion of Q2. This problem was discussed in the context of ALTADENA, but it is also very important for magnetic field variation e.g. in PHIP-SAH. Let us consider a simple ABX system. At low fields, when proton chemical shift difference can be neglected, the ABX system becomes equivalent to an A₂X system meaning that for protons S-T basis is more appropriate at low fields. $\sigma_S^{A,B}$ is the initial state of the system after pH₂ addition ($\sigma_{\text{initial}} = \sigma_S^{A,B}$). Then, we increase the field slowly so that the system changes from A₂X to ABX and basis from S-T to Zeeman. This means that the symmetry basis of the system before and after (and during!) the transformation is different. The theory presented here can not be applied.

Although in three-spin systems, we can still reach 100% X nuclear polarization, we again could underestimate the efficiency of polarization transfer in more complex systems.

It looks as if the methodology used here for the static high magnetic field can be translated to the low fields (and zero fields). However, the basis will be system symmetry specific and, in addition, will depend on the J -coupling network.

Assessing the validity of this approach is not straight forward. To date, however, experimental results have not contradicted the calculated results presented here.

5. Conclusion

The mathematical framework presented here allows to determine an upper limit for the polarization transfer from pH_2 to X-nuclei or other protons with an emphasis on the effect of molecular of spin symmetry. Solutions were presented for the most current experimental situations, although some more complex cases remain unaddressed. This method may serve as a first check to estimate if and how much polarization transfer is possible in a given situation. Naturally, identifying and optimization a dedicated transfer strategy is the following essential step which is not addressed here.

Supplementary Materials: All used Matlab scripts together with MOIN spin library [60] (.zip) are available online or on request.

Author Contributions: ANP conceptualization, software, DAB visualization, ANP, DAB original draft, ANP, DAB, IVK investigation, All review and editing, funding acquisition. All authors have read and agreed to the published version of the manuscript.

Acknowledgments and funding: We acknowledge funding from German Federal Ministry of Education and Research (BMBF) within the framework of the e:Med research and funding concept (01ZX1915C), DFG (PR 1868/3-1, HO-4602/2-2, HO-4602/3, GRK2154-2019, EXC2167, FOR5042, SFB1479, TRR287), Kiel University and the Faculty of Medicine. MOIN CC was founded by a grant from the European Regional Development Fund (ERDF) and the Zukunftsprogramm Wirtschaft of Schleswig-Holstein (Project no. 122-09-053). DAB acknowledges support from the Alexander von Humboldt Foundation in the framework of the Sofja Kovalevskaja Award. I.V.K. acknowledges the Russian Ministry of Science and Higher Education (grant no. 075-15-2020-779 and 075-15-2021-580) for financial support. We are grateful to Dmitry Budker for the discussion and editing of the manuscript.

Conflicts of Interest: The authors declare no conflict of interest.

Appendix A

1. A_2 two spin- $1/2$ system, C_2 group

The number of states is $2^2=4$.

The basis for two equivalent spins can be divided into two groups with total spin I^{tot} of 1 (three states) and 0 (one state) also known as singlet-triplet (S-T) basis. This can be derived formally by finding eigenfunctions and eigenvalues (λ) of cyclic permutation operator $\begin{pmatrix} 12 \\ 21 \end{pmatrix} = (21)$. C_2 permutation group of A_2 system consists of two permutations, $\{(),(21)\}$. In the matrix form written in the Zeeman basis $(|\alpha\alpha\rangle, |\alpha\beta\rangle, |\beta\alpha\rangle, |\beta\beta\rangle)$:

$$\begin{aligned} () = E &= \begin{pmatrix} 1 & 0 & 0 & 0 \\ 0 & 1 & 0 & 0 \\ 0 & 0 & 1 & 0 \\ 0 & 0 & 0 & 1 \end{pmatrix}, \\ (21) = C_2 &= \begin{pmatrix} 1 & 0 & 0 & 0 \\ 0 & 0 & 1 & 0 \\ 0 & 1 & 0 & 0 \\ 0 & 0 & 0 & 1 \end{pmatrix}. \end{aligned} \tag{A1}$$

Eigenvalues of C_2 are given as a superscript to the corresponding wavefunctions:

$$\begin{aligned} \lambda = 1, \text{ group } 1 \in A \\ |1, +1\rangle^1 = |T_+\rangle = |\alpha\alpha\rangle, \\ |1, 0\rangle^1 = |T_0\rangle = \frac{|\alpha\beta\rangle + |\beta\alpha\rangle}{\sqrt{2}}, \end{aligned} \tag{A2}$$

$$|1, -1\rangle^1 = |T_-\rangle = |\beta\beta\rangle,$$

$$\lambda = -1, \text{ group } 2 \in B$$

$$|0,0\rangle^{-1} = |S_0\rangle = \frac{|\alpha\beta\rangle - |\beta\alpha\rangle}{\sqrt{2}}.$$

We indicate spin states by the total spin I^{tot} and its projection I_Z^{tot} as $|I^{\text{tot}}, I_Z^{\text{tot}}\rangle^\lambda$ and/or by using Zeeman basis, $|\alpha\rangle$ and $|\beta\rangle$.

Table A1. Table of characters for A_2 two spin- $1/2$ system (C_2 group).

	E	C_2
A	1	1
B	1	-1
SpinRep = 3A + B	4	2

Therefore, there are three symmetric and one asymmetric states with respect to (12) permutation (or rotation about 180 degrees, C_2). It follows from both eq A1 and Table A1. Therefore, the basis for A_2 two spin- $1/2$ system consists of 2 sets (S) with multiplicity 3 and 1 (SpinRep = 3A + B):

$$\begin{aligned} S_A^{12} &= \{|T_+\rangle, |T_0\rangle, |T_-\rangle\}, \\ S_B^{12} &= \{|S_0\rangle\}. \end{aligned} \quad (\text{A3})$$

To calculate characters for spin permutations (SpinRep) in Table A1, one can (i) write matrix of permutation and (ii) calculate trace. For an identity transformation, $()=E$, for N spin- $1/2$ character is

$$\chi_{\text{SpinRep}}(E) = \text{Tr}(E) = 2^N. \quad (\text{A4})$$

Analogously (eq A1) $\chi_{\text{SpinRep}}(C_2) = \text{Tr}(C_2) = 2$.

For any character X of a representation $T = \bigoplus_i T_i$ which is superposition of irreducible representations of the same group, the multiplicity n_k of the irreducible representation T_i is given by

$$n_k = \frac{1}{\Omega_G} \sum_g X(g)^* \chi_k(g). \quad (\text{A5})$$

Here "*" is a complex conjugate and $\Omega_G = \sum_g \chi_k(g)^* \chi_k(g)$. Eq A5 is useful to decompose the SpinRep line into a sum of characters for irreducible representations. So, for A_2 system SpinRep = 3A + B.

2. A_3 three spin- $1/2$ system, C_3 group

The number of states is $2^3 = 8$.

The basis of three equivalent spins can be grouped on three groups with total spin I^{tot} of 3/2 (4 states), 1/2 (2 states) and 1/2 (2 states). Here also to distinguish groups, we introduce eigenvalues for cycling permutation operator $\begin{pmatrix} 123 \\ 231 \end{pmatrix} = (231)$ and its values are given as a superscript to the corresponding wavefunctions.

$$I^{\text{tot}} = 3/2, \lambda = 1, \text{ group } 1 \in A$$

$$\left| \frac{3}{2}, +\frac{3}{2} \right\rangle^1 = |\alpha\alpha\alpha\rangle,$$

$$\left| \frac{3}{2}, +\frac{1}{2} \right\rangle^1 = \frac{1}{\sqrt{3}}(|\alpha\alpha\beta\rangle + |\alpha\beta\alpha\rangle + |\beta\alpha\alpha\rangle),$$

$$\left| \frac{3}{2}, -\frac{1}{2} \right\rangle^1 = \frac{1}{\sqrt{3}}(|\alpha\beta\beta\rangle + |\beta\alpha\beta\rangle + |\beta\beta\alpha\rangle)$$

$$\left| \frac{3}{2}, -\frac{3}{2} \right\rangle^1 = |\beta\beta\beta\rangle, \quad (\text{A6})$$

$$I^{\text{tot}} = 1/2, \lambda = e^{\frac{i2\pi}{3}} = e^{+i\theta}, \text{ group } 2 \in E_1$$

$$\left| \frac{1}{2}, +\frac{1}{2} \right\rangle^{e^{+i\theta}} = \frac{|\alpha\alpha\beta\rangle + e^{-i\theta}|\alpha\beta\alpha\rangle + e^{+i\theta}|\beta\alpha\alpha\rangle}{\sqrt{3}},$$

$$\left| \frac{1}{2}, -\frac{1}{2} \right\rangle^{e^{+i\theta}} = \frac{|\beta\beta\alpha\rangle + e^{-i\theta}|\beta\alpha\beta\rangle + e^{+i\theta}|\alpha\beta\beta\rangle}{\sqrt{3}},$$

$$I^{\text{tot}} = 1/2, \lambda = e^{-\frac{i2\pi}{3}} = e^{-i\theta}, \text{ group } 3 \in E_2$$

$$\left| \frac{1}{2}, +\frac{1}{2} \right\rangle^{e^{-i\theta}} = \frac{|\alpha\alpha\beta\rangle + e^{+i\theta}|\alpha\beta\alpha\rangle + e^{-i\theta}|\beta\alpha\alpha\rangle}{\sqrt{3}},$$

$$\left| \frac{1}{2}, -\frac{1}{2} \right\rangle^{e^{-i\theta}} = \frac{|\beta\beta\alpha\rangle + e^{+i\theta}|\beta\alpha\beta\rangle + e^{-i\theta}|\alpha\beta\beta\rangle}{\sqrt{3}}.$$

The C_3 permutation group $G = \left\{ \begin{pmatrix} 123 \\ 123 \end{pmatrix}, \begin{pmatrix} 123 \\ 231 \end{pmatrix}, \begin{pmatrix} 123 \\ 312 \end{pmatrix} \right\} = \{0, (+\theta), (-\theta)\}$ of A_3 system consists of three permutations: the trivial identity permutation, permutation or "+ θ " rotation and "- θ " rotation, with $\theta = \frac{2\pi}{3}$.

Table A2. Table of characters for A_3 three spin- $1/2$ system (C_3 group). Here $\theta = \frac{2\pi}{3}$. Note the difference between three different "E" here. The characters for spin representations (SpinRep) are filled using eq A4 and following discussions. Any permutation (or rotation) will leave only states $|\alpha\alpha\alpha\rangle$ and $|\beta\beta\beta\rangle$ on the diagonal. It means that the sum of diagonal elements and corresponding character value is 2.

	E	C_3^1	C_3^2
A	1	1	1
E₁	1	$e^{i\theta}$	$e^{-i\theta}$
E₂	1	$e^{-i\theta}$	$e^{i\theta}$
SpinRep = 4A + 2E₁+2E₂	8	2	2

Summarizing, there are 4 symmetric (g) states and two pairs of rotationally symmetric states (E_i, |S>) states. It follows from both: eq A6 and Table A2. Therefore, the basis for A_3 three spin- $1/2$ system consists of 3 sets with multiplicity 4, 2 and 2 (SpinRep = 4A + 2E₁+2E₂):

$$\begin{aligned} S_A^{123} &= \left\{ \left| \frac{3}{2}, +\frac{3}{2} \right\rangle^1, \left| \frac{3}{2}, +\frac{1}{2} \right\rangle^1, \left| \frac{3}{2}, -\frac{1}{2} \right\rangle^1, \left| \frac{3}{2}, -\frac{3}{2} \right\rangle^1 \right\}, \\ S_{E_1}^{123} &= \left\{ \left| \frac{1}{2}, +\frac{1}{2} \right\rangle^{e^{+i\theta}}, \left| \frac{1}{2}, -\frac{1}{2} \right\rangle^{e^{+i\theta}} \right\}, \\ S_{E_2}^{123} &= \left\{ \left| \frac{1}{2}, +\frac{1}{2} \right\rangle^{e^{-i\theta}}, \left| \frac{1}{2}, -\frac{1}{2} \right\rangle^{e^{-i\theta}} \right\} \end{aligned} \quad (\text{A7})$$

3. A_4 four spin- $1/2$ system: C_4 group example

The number of states is $2^4 = 16$.

The basis of four spins can be grouped on 4 groups with total spin I^{tot} of 2 (five states), 1 (3 groups, each consists of 3 states), and 0 (two groups, each one state).

C_4 permutation group $G = \left\{ \begin{pmatrix} 1234 \\ 1234 \end{pmatrix}, \begin{pmatrix} 1234 \\ 2341 \end{pmatrix}, \begin{pmatrix} 1234 \\ 3412 \end{pmatrix}, \begin{pmatrix} 1234 \\ 4123 \end{pmatrix} \right\} = \{0, (2341), (3412), (4123)\}$ of A_4 system consists of four permutations: () – trivial identity permutation and three cyclic permutations that are equivalent to rotation of a square by 90°, 180° and 270° around the center axis perpendicular to its plane. Note that only 180° rotation can be represented as two consequent permutations (3412) = (13)(24).

Table A3. Table of characters for A_4 four spin- $1/2$ system (C_4 group). The characters for SpinRep are filled using eq A4 and following discussion. Any rotations will leave states $|\alpha\alpha\alpha\alpha\rangle$ and $|\beta\beta\beta\beta\rangle$ on diagonal. All other states are changing after an odd number of cyclic permutations. Hence, character for C_4 and $(C_4)^3$ is only 2. 180° rotation ((13)(24) permutation) does not change also $|\alpha\beta\alpha\beta\rangle$ and $|\beta\alpha\beta\alpha\rangle$ states. Hence the corresponding character is 2+2=4. It means that the sum of diagonal elements and corresponding character values are 4 for each rotation (permutation).

	E	C_4	$C_2 = (C_4)^2$	$(C_4)^3$
A	+1	+1	+1	+1
B	+1	-1	+1	-1

E₁	+1	+i	-1	-i
E₂	+1	-i	-1	+i
SpinRep = 6A + 4B+3E₁+3E₂	16	2	4	2

4. AA'(AA') four spin-1/2 system: D₂ group (spin symmetry of ethylene)

The number of states is 2⁴ = 16.

The basis of four spins can be grouped into 4 groups with total spin I^{tot} of 2 (five states), 1 (3 groups, each consists of 3 states), and 0 (two groups, each one state).

D₂ permutation group $G = \left\{ \begin{pmatrix} 1234 \\ 1234 \end{pmatrix}, \begin{pmatrix} 1234 \\ 2143 \end{pmatrix}, \begin{pmatrix} 1234 \\ 3412 \end{pmatrix}, \begin{pmatrix} 1234 \\ 4321 \end{pmatrix} \right\} = \{(), (21)(43), (31)(42), (41)(32)\}$ of AA'(AA') system consists of four permutations: () – trivial identity permutation and three pairwise permutations that are equivalent to rotations of the rectangle by 180° around three orthogonal axes, which are orthogonal to the plane of the rectangle and (or) its edges. We do not write here corresponding basis for general D₂ group which is equivalent to D_{2h} discussed below.

Table A4. Table of characters for AA'(AA') four spin-1/2 system (D₂ group). The characters for SpinRep are filled using eq A4 and following discussion. Any rotations will leave states $|aaaa\rangle$ and $|\beta\beta\beta\beta\rangle$ on diagonal. In addition, states $|\alpha\alpha\beta\beta\rangle$ and $|\beta\beta\alpha\alpha\rangle$ do not change by the action of (21)(43) permutation. For two other rotations, one can also write the corresponding two states. It means that the sum of diagonal elements and corresponding character values are 4 for each rotation (permutation).

	E	C₂(z)	C₂(y)	C₂(x)
A	+1	+1	+1	+1
B₁	+1	+1	-1	-1
B₂	+1	-1	+1	-1
B₃	+1	-1	-1	+1
SpinRep = 7A + 3B₁+3B₂+3B₃	16	4	4	4

5. AA' (AA') four spin-1/2 system, D_{2h} group (molecular symmetry of ethylene)[19]

The number of states is 2⁴ = 16.

The basis of four spins can be grouped into 4 groups with total spin I^{tot} of 2 (five states), 1 (3 groups, each consists of 3 states), and 0 (two groups, each one state).

D_{2h} group is a direct product of D₂ and C_i groups. D₂ part consists of 4 spin permutations $G(D_2) = \{(), (12)(34), (13)(24), (14)(23)\}$. An addition of inversion operator of C_i results in four additional transformations $\{i, \sigma(xy), \sigma(xz), \sigma(yz)\}$: inversion "i" and three mirror σ -planes: xy, xz or yz (**Figure A1 and 4**).

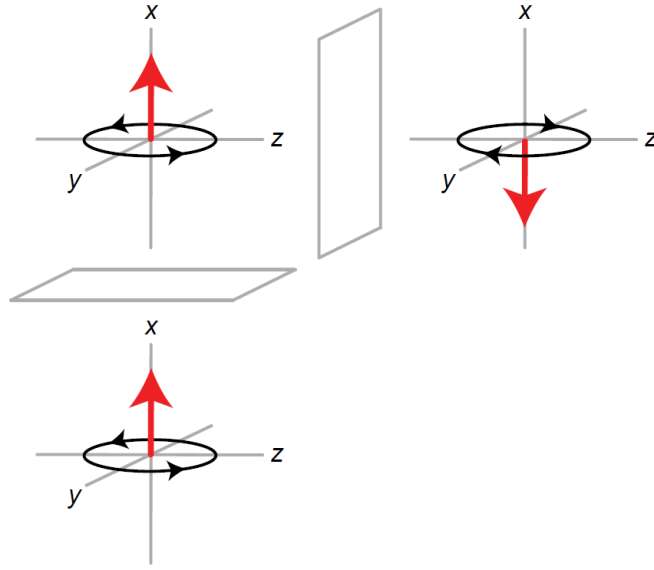


Figure A1. Action of a mirror plane on an axial vector (spin or magnetic dipole). When axial vector is perpendicular to the mirror plane, it does not change upon reflection. If, however, it is oriented along the mirror plane, it changes its orientation upon reflection.[61]

The eigenvectors for ethylene were found before[19] and are given in eq (A10) without change.

$$I^{tot} = 2, \text{ group 1} \in A_g$$

$$|2, +2\rangle^g = |\alpha\alpha\alpha\rangle,$$

$$|2, +1\rangle^g = \frac{|\alpha\alpha\alpha\beta\rangle + |\alpha\alpha\beta\alpha\rangle + |\alpha\beta\alpha\alpha\rangle + |\beta\alpha\alpha\alpha\rangle}{2},$$

$$|2, 0\rangle^g = \frac{|\alpha\alpha\beta\beta\rangle + |\alpha\beta\alpha\beta\rangle + |\alpha\beta\beta\alpha\rangle + |\beta\alpha\beta\alpha\rangle + |\beta\beta\alpha\alpha\rangle + |\beta\alpha\alpha\beta\rangle}{\sqrt{6}},$$

$$|2, -1\rangle^g = \frac{|\beta\beta\beta\alpha\rangle + |\beta\beta\alpha\beta\rangle + |\beta\alpha\beta\beta\rangle + |\alpha\beta\beta\beta\rangle}{2},$$

$$|2, -2\rangle^g = |\beta\beta\beta\beta\rangle,$$

$$I^{tot} = 1, \text{ group 2} \in B_{1u}$$

$$|1, +1\rangle^{1u} = \frac{-|\alpha\alpha\alpha\beta\rangle - |\alpha\alpha\beta\alpha\rangle + |\alpha\beta\alpha\alpha\rangle + |\beta\alpha\alpha\alpha\rangle}{2},$$

$$|1, 0\rangle^{1u} = \frac{|\alpha\alpha\beta\beta\rangle - |\beta\beta\alpha\alpha\rangle}{\sqrt{2}},$$

$$|1, -1\rangle^{1u} = \frac{|\beta\beta\beta\alpha\rangle + |\beta\beta\alpha\beta\rangle - |\beta\alpha\beta\beta\rangle - |\alpha\beta\beta\beta\rangle}{2}$$

$$I^{tot} = 1, \text{ group 3} \in B_{2u}$$

$$|1, +1\rangle^{2u} = \frac{|\alpha\alpha\alpha\beta\rangle - |\alpha\alpha\beta\alpha\rangle + |\alpha\beta\alpha\alpha\rangle - |\beta\alpha\alpha\alpha\rangle}{2},$$

$$|1, 0\rangle^{2u} = \frac{|\alpha\beta\alpha\beta\rangle - |\beta\alpha\beta\alpha\rangle}{\sqrt{2}},$$

$$|1, -1\rangle^{2u} = \frac{-|\beta\beta\beta\alpha\rangle + |\beta\beta\alpha\beta\rangle - |\beta\alpha\beta\beta\rangle + |\alpha\beta\beta\beta\rangle}{2}$$

$$I^{tot} = 1, \text{ group 4} \in B_{3g}$$

$$|1, +1\rangle^{3g} = \frac{-|\alpha\alpha\alpha\beta\rangle + |\alpha\alpha\beta\alpha\rangle + |\alpha\beta\alpha\alpha\rangle - |\beta\alpha\alpha\alpha\rangle}{2},$$

$$|1, 0\rangle^{3g} = \frac{|\beta\alpha\alpha\beta\rangle - |\alpha\beta\beta\alpha\rangle}{\sqrt{2}},$$

$$|1, -1\rangle^{3g} = \frac{-|\beta\beta\beta\alpha\rangle + |\beta\beta\alpha\beta\rangle + |\beta\alpha\beta\beta\rangle - |\alpha\beta\beta\beta\rangle}{2}$$

$$I^{tot} = 0, \text{ group 5} \in A_g$$

$$|0, 0\rangle^{g,s1} = \frac{-\kappa|\beta\beta\alpha\alpha\rangle + |\beta\alpha\beta\alpha\rangle + (\kappa-1)|\beta\alpha\alpha\beta\rangle + (\kappa-1)|\alpha\beta\beta\alpha\rangle + |\alpha\beta\alpha\beta\rangle - \kappa|\alpha\alpha\beta\beta\rangle}{2\sqrt{1-\kappa+\kappa^2}},$$

(A10)

$I^{tot} = 0$, group 6 $\in A_g$

$$|0,0\rangle_{g,s2} = \frac{(\kappa-2)|\beta\beta\alpha\alpha\rangle - (2\kappa-1)|\beta\alpha\beta\alpha\rangle + (\kappa+1)|\beta\alpha\alpha\beta\rangle + (\kappa+1)|\alpha\beta\beta\alpha\rangle - (2\kappa-1)|\alpha\beta\alpha\beta\rangle + (\kappa-2)|\alpha\alpha\beta\beta\rangle}{2\sqrt{3}\sqrt{1-\kappa+\kappa^2}}$$

$$\text{with } \kappa = \frac{\sqrt{J_g^2 + J_c^2 + J_t^2 - (J_g J_c + J_g J_t + J_c J_t)} + (J_g - J_c)}{J_g - J_t}$$

It is not as trivial as before to fill the SpinRep line in the character **Table A5** as in the previous cases; this needs some elaboration. However, the first four elements are identical to the one from **Table A4** for group D_2 .

Let's consider mirror plane $\sigma(yz)$ (**Figure 1A**), that also can be referred to as σ_h . It does not change the position of atoms (a) and because spin is an axial vector (b) the spin states do not change under the action of $\sigma(yz)$. Hence the corresponding character is 16 (number of spin states). We refer to this operator as parity in the main text, and it changes sign of one coordinate axis (here x).

Now, let's consider two mirror planes $\sigma(xy)$ and $\sigma(xz)$ (**Figure 1A**), also referred to as σ_v . σ_v exchanges two neighbor protons (permutations (12)(34) or (14)(23)) and changes sign of the spin projection (it is not convenient for NMR but using this notation of axis, we assume the projections of the spin states along x axis). So, when two pairs of protons are exchanged and their sign is inverted, then there are only 4 states what do not change under the action of this transformation: $|\alpha\beta\alpha\beta\rangle$, $|\beta\alpha\alpha\beta\rangle$, $|\beta\alpha\beta\alpha\rangle$ and $|\alpha\beta\beta\alpha\rangle$ for the case of (12)(34) permutation with inversion. Analogous 4 states can be written for the other mirror transformation. Hence the two corresponding characters are 4.

And finally, inversion i . It exchanges the protons as (13)(24) (a) and changes sign of the spin projections, meaning that only four states $|\alpha\alpha\beta\beta\rangle$, $|\beta\beta\alpha\alpha\rangle$, $|\beta\alpha\alpha\beta\rangle$ and $|\alpha\beta\beta\alpha\rangle$ will stay the same; hence the corresponding character is 4.

Table A5. Table of characters for AA' (AA') four spin-1/2 system (D_{2h} group). This can be obtained as a direct product of C_i (the same as C_2) and D_2 character groups. See text how to fill SpinRep line.

	E	$C_2(z)$	$C_2(y)$	$C_2(x)$	i	$\sigma(xy)$	$\sigma(xz)$	$\sigma(yz)$
A_g	+1	+1	+1	+1	+1	+1	+1	+1
B_{1g}	+1	+1	-1	-1	+1	+1	-1	-1
B_{2g}	+1	-1	+1	-1	+1	-1	+1	-1
B_{3g}	+1	-1	-1	+1	+1	-1	-1	+1
A_u	+1	+1	+1	+1	-1	-1	-1	-1
B_{1u}	+1	+1	-1	-1	-1	-1	+1	+1
B_{2u}	+1	-1	+1	-1	-1	+1	-1	+1
B_{3u}	+1	-1	-1	+1	-1	+1	+1	-1
SpinRep = 7A_g + 3B_{1u} + 3B_{2u} + 3B_{3u}	16	4	4	4	4	4	4	16

There are 7 symmetrical (A_g symmetry) states, and three states for each of three B symmetries (B_{1u} , B_{2u} and B_{3u}). This follows from both eq (A10) and **Table A5**. Therefore, the basis for AA' (AA') four spin-1/2 system of D_{2h} symmetry consists of 4 sets with multiplicity 7, 3, 3 and 3 (Spins rep. = $7A_g + 3B_{1u} + 3B_{2u} + 3B_{3u}$):

$$\begin{aligned} S_{A_g}^{D_{2h}} &= \{|2, +2\rangle^g, |2, +1\rangle^g, |2, 0\rangle^g, |2, -1\rangle^g, |2, -2\rangle^g, |0, 0\rangle^{g,s1}, |0, 0\rangle^{g,s2}\}, \\ S_{B_{1u}}^{D_{2h}} &= \{|1, +1\rangle^{1u}, |1, 0\rangle^{1u}, |1, -1\rangle^{1u}\}, \\ S_{B_{2u}}^{D_{2h}} &= \{|1, +1\rangle^{2u}, |1, 0\rangle^{2u}, |1, -1\rangle^{2u}\}, \\ S_{B_{3u}}^{D_{2h}} &= \{|1, +1\rangle^{3u}, |1, 0\rangle^{3u}, |1, -1\rangle^{3u}\} \end{aligned} \tag{A11}$$

Note that in the case of C_4 symmetry considered earlier, six states belong to the $A_{(g)}$ group.

Appendix B

Table B1. Maximum expected polarization transfer coefficient ξ_{\max} for systems without symmetry constraints and for pHz derived spin order transfer (states $\sigma_{ZZ}^{A,B}$ or $\sigma_S^{A,B}$) to the longitudinal polarization of all protons of the same molecule (average polarization).

Type of the system	Number of spins	ξ_{\max} from $\sigma_{ZZ}^{A,B} = \xi\sigma_P^X + \sigma_{\text{rest}}$	ξ_{\max} from $\sigma_S^{A,B} = \xi\sigma_P^X + \sigma_{\text{rest}}$
AB	2	1/2	1
ABC	3	1/2	2/3
ABCD	4	3/8	5/8
ABCDE	5	3/8	11/20
ABCDEF	6	5/16	1/2
ABCDEFG	7	5/16	0.4821
ABCDEFGH	8	0.2734	0.4336
ABCDEFGHI	9	0.2734	0.4323
ABCDEFGHIJ	10	0.2461	0.3906
ABCDEFGHIJK	11	0.2461	0.3835
ABCDEFGHIJKL	12	0.2256	0.3597

Table B2. Maximum expected polarization transfer coefficient ξ_{\max}^{SC} for systems with symmetry constraints and for pHz derived spin order transfer (state $\sigma_S^{A,B}$) to the longitudinal polarization of all protons of the same molecule (average polarization).

Type of the system	Number of spins	ξ_{\max}^{SC} from $\sigma_S^{A,B} = \xi\sigma_P^X + \sigma_{\text{rest}}$
A ₂ B	3	1/3
A ₂ BC	4	0.3125
A ₃ B	4	0.25
A ₂ B ₂	4	0.1875
A ₃ BC	5	0.175
A ₂ B ₂ C	5	0.175
A ₃ B ₂	5	0.1167
A ₃ BCD	6	0.2014
A ₃ B ₂ C	6	0.1424
A ₃ B ₃	6	0.1204

References

1. Natterer, J.; Bargon, J. Parahydrogen Induced Polarization. *Prog. Nucl. Magn. Reson. Spectrosc.* **1997**, *31*, 293–315, doi:10.1016/S0079-6565(97)00007-1.
2. Green, R.A.; Adams, R.W.; Duckett, S.B.; Mewis, R.E.; Williamson, D.C.; Green, G.G.R. The Theory and Practice of Hyperpolarization in Magnetic Resonance Using Parahydrogen. *Prog. Nucl. Magn. Reson. Spectrosc.* **2012**, *67*, 1–48, doi:10.1016/j.pnmrs.2012.03.001.
3. Ellermann, F.; Pravdivtsev, A.; Hövener, J.-B. Open-Source, Partially 3D-Printed, High-Pressure (50-Bar) Liquid-Nitrogen-Cooled Parahydrogen Generator. *Magn. Reson.* **2021**, *2*, 49–62, doi:https://doi.org/10.5194/mr-2-49-2021.

-
4. Hövener, J.-B.; Bär, S.; Leupold, J.; Jenne, K.; Leibfritz, D.; Hennig, J.; Duckett, S.B.; von Elverfeldt, D. A Continuous-Flow, High-Throughput, High-Pressure Parahydrogen Converter for Hyperpolarization in a Clinical Setting. *NMR Biomed.* **2013**, *26*, 124–131, doi:10.1002/nbm.2827.
 5. Feng, B.; Coffey, A.M.; Colon, R.D.; Chekmenev, E.Y.; Waddell, K.W. A Pulsed Injection Parahydrogen Generator and Techniques for Quantifying Enrichment. *J. Magn. Reson.* **2012**, *214*, 258–262, doi:10.1016/j.jmr.2011.11.015.
 6. Bowers, C.R.; Weitekamp, D.P. Parahydrogen and Synthesis Allow Dramatically Enhanced Nuclear Alignment. *J. Am. Chem. Soc.* **1987**, *109*, 5541–5542, doi:10.1021/ja00252a049.
 7. Pravica, M.G.; Weitekamp, D.P. Net NMR Alignment by Adiabatic Transport of Parahydrogen Addition Products to High Magnetic Field. *Chem. Phys. Lett.* **1988**, *145*, 255–258, doi:10.1016/0009-2614(88)80002-2.
 8. Adams, R.W.; Aguilar, J.A.; Atkinson, K.D.; Cowley, M.J.; Elliott, P.I.P.; Duckett, S.B.; Green, G.G.R.; Khazal, I.G.; López-Serrano, J.; Williamson, D.C. Reversible Interactions with Para-Hydrogen Enhance NMR Sensitivity by Polarization Transfer. *Science* **2009**, *323*, 1708–1711, doi:10.1126/science.1168877.
 9. Korchak, S.; Mamone, S.; Glöggl, S. Over 50 % ¹H and ¹³C Polarization for Generating Hyperpolarized Metabolites—A Para-Hydrogen Approach. *ChemistryOpen* **2018**, *7*, 672–676, doi:10.1002/open.201800086.
 10. Hövener, J.-B.; Schwaderlapp, N.; Borowiak, R.; Lickert, T.; Duckett, S.B.; Mewis, R.E.; Adams, R.W.; Burns, M.J.; Highton, L.A.R.; Green, G.G.R.; et al. Toward Biocompatible Nuclear Hyperpolarization Using Signal Amplification by Reversible Exchange: Quantitative in Situ Spectroscopy and High-Field Imaging. *Anal. Chem.* **2014**, *86*, 1767–1774, doi:10.1021/ac403653q.
 11. Buckenmaier, K.; Scheffler, K.; Plaumann, M.; Fehling, P.; Bernarding, J.; Rudolph, M.; Back, C.; Koelle, D.; Kleiner, R.; Hövener, J.-B.; et al. Multiple Quantum Coherences Hyperpolarized at Ultra-Low Fields. *ChemPhysChem* **2019**, *20*, 2823–2829, doi:10.1002/cphc.201900757.
 12. Glöggl, S.; Müller, R.; Colell, J.; Emondts, M.; Dabrowski, M.; Blümich, B.; Appelt, S. Para-Hydrogen Induced Polarization of Amino Acids, Peptides and Deuterium–Hydrogen Gas. *Phys. Chem. Chem. Phys.* **2011**, *13*, 13759–13764, doi:10.1039/C1CP20992B.
 13. Barskiy, D.A.; Tayler, M.C.D.; Marco-Rius, I.; Kurhanewicz, J.; Vigneron, D.B.; Cikrikci, S.; Aydogdu, A.; Reh, M.; Pravdivtsev, A.N.; Hövener, J.-B.; et al. Zero-Field Nuclear Magnetic Resonance of Chemically Exchanging Systems. *Nat. Commun.* **2019**, *10*, 3002, doi:10.1038/s41467-019-10787-9.
 14. Levitt, M.H. Symmetry Constraints on Spin Dynamics: Application to Hyperpolarized NMR. *J. Magn. Reson.* **2016**, *262*, 91–99, doi:10.1016/j.jmr.2015.08.021.
 15. Ivanov, K.L.; Pravdivtsev, A.N.; Yurkovskaya, A.V.; Vieth, H.-M.; Kaptein, R. The Role of Level Anti-Crossings in Nuclear Spin Hyperpolarization. *Prog. Nucl. Magn. Reson. Spectrosc.* **2014**, *81*, 1–36, doi:10.1016/j.pnmrs.2014.06.001.
 16. Bhattacharya, P.; Harris, K.; Lin, A.P.; Mansson, M.; Norton, V.A.; Perman, W.H.; Weitekamp, D.P.; Ross, B.D. Ultra-Fast Three Dimensional Imaging of Hyperpolarized ¹³C in Vivo. *Magn. Reson. Mater. Phys.* **2005**, *18*, 245–256, doi:10.1007/s10334-005-0007-x.
 17. Schmidt, A.B.; Berner, S.; Braig, M.; Zimmermann, M.; Hennig, J.; Elverfeldt, D. von; Hövener, J.-B. In Vivo ¹³C-MRI Using SAMBADENA. *PLOS ONE* **2018**, *13*, e0200141, doi:10.1371/journal.pone.0200141.
 18. Svyatova, A.; Skovpin, I.V.; Chukanov, N.V.; Kovtunov, K.V.; Chekmenev, E.Y.; Pravdivtsev, A.N.; Hövener, J.-B.; Koptuyug, I.V. ¹⁵N MRI of SLIC-SABRE Hyperpolarized ¹⁵N-Labelled Pyridine and Nicotinamide. *Chem. Eur. J.* **2019**, *25*, 8465–8470, doi:10.1002/chem.201900430.
 19. Zhivonitko, V.V.; Kovtunov, K.V.; Chapovsky, P.L.; Koptuyug, I.V. Nuclear Spin Isomers of Ethylene: Enrichment by Chemical Synthesis and Application for NMR Signal Enhancement. *Angew. Chem. Int. Ed.* **2013**, *52*, 13251–13255, doi:10.1002/anie.201307389.

-
20. Cavallari, E.; Carrera, C.; Aime, S.; Reineri, F. Metabolic Studies of Tumor Cells Using [1-13C] Pyruvate Hyperpolarized by Means of PHIP-Side Arm Hydrogenation. *ChemPhysChem* **2019**, *20*, 318–325, doi:10.1002/cphc.201800652.
 21. Sellies, L.; Aspers, R.; Feiters, M.C.; Rutjes, F.; Tessari, M. Para-Hydrogen Hyperpolarization Allows Direct NMR Detection of α -Amino Acids in Complex (Bio)Mixtures. *Angew. Chem. Int. Ed. n/a*, doi:10.1002/anie.202109588.
 22. Nielsen, N.C.; Sorensen, O.W. Conditional Bounds on Polarization Transfer. *J. Magn. Reson. A* **1995**, *114*, 24–31, doi:10.1006/jmra.1995.1101.
 23. Nielsen, N.C.; Schulte-Herbrüggen, T.; Sørensen, O.W. Bounds on Spin Dynamics Tightened by Permutation Symmetry Application to Coherence Transfer in I2S and I3S Spin Systems. *Mol. Phys.* **1995**, *85*, 1205–1216, doi:10.1080/00268979500101771.
 24. Sengstschmid, H.; Freeman, R.; Barkemeyer, J.; Bargon, J. A New Excitation Sequence to Observe the PASADENA Effect. *J. Magn. Reson. A* **1996**, *120*, 249–257, doi:10.1006/jmra.1996.0121.
 25. Kiryutin, A.S.; Ivanov, K.L.; Yurkovskaya, A.V.; Vieth, H.-M.; Lukzen, N.N. Manipulating Spin Hyperpolarization by Means of Adiabatic Switching of a Spin-Locking RF-Field. *Phys. Chem. Chem. Phys.* **2013**, *15*, 14248–14255, doi:10.1039/C3CP52061G.
 26. Pravdivtsev, A.N.; Yurkovskaya, A.V.; Petrov, P.A.; Vieth, H.-M. Coherent Evolution of Singlet Spin States in PHOTO-PHIP and M2S Experiments. *Phys. Chem. Chem. Phys.* **2017**, *19*, 25961–25969, doi:10.1039/C7CP04122E.
 27. Pravdivtsev, A.N.; Kiryutin, A.S.; Yurkovskaya, A.V.; Vieth, H.-M.; Ivanov, K.L. Robust Conversion of Singlet Spin Order in Coupled Spin-1/2 Pairs by Adiabatically Ramped RF-Fields. *J. Magn. Reson.* **2016**, *273*, 56–64, doi:10.1016/j.jmr.2016.10.003.
 28. Pravdivtsev, A.N.; Sönnichsen, F.; Hövener, J.-B. OnlyParahydrogen Spectroscopy (OPSY) Pulse Sequences – One Does Not Fit All. *J. Magn. Reson.* **2018**, *297*, 86–95, doi:10.1016/j.jmr.2018.10.006.
 29. Aguilar, J.A.; Adams, R.W.; Duckett, S.B.; Green, G.G.R.; Kandiah, R. Selective Detection of Hyperpolarized NMR Signals Derived from Para-Hydrogen Using the Only Para-Hydrogen Spectroscopy (OPSY) Approach. *J. Magn. Reson.* **2011**, *208*, 49–57, doi:10.1016/j.jmr.2010.10.002.
 30. Ratajczyk, T.; Gutmann, T.; Dillenberger, S.; Abdulhussaein, S.; Frydel, J.; Breitzke, H.; Bommerich, U.; Trantschel, T.; Bernarding, J.; Magusin, P.C.M.M.; et al. Time Domain Para Hydrogen Induced Polarization. *Solid State Nucl. Magn. Reson.* **2012**, *43–44*, 14–21, doi:10.1016/j.ssnmr.2012.02.002.
 31. Buntkowsky, G.; Gutmann, T.; Petrova, M.V.; Ivanov, K.L.; Bommerich, U.; Plaumann, M.; Bernarding, J. Dipolar Induced Para-Hydrogen-Induced Polarization. *Solid State Nucl. Magn. Reson.* **2014**, *63–64*, 20–29, doi:10.1016/j.ssnmr.2014.07.002.
 32. Stevanato, G.; Hill-Cousins, J.T.; Håkansson, P.; Roy, S.S.; Brown, L.J.; Brown, R.C.D.; Pileio, G.; Levitt, M.H. A Nuclear Singlet Lifetime of More than One Hour in Room-Temperature Solution. *Angew. Chem. Int. Ed.* **2015**, *54*, 3740–3743, doi:10.1002/anie.201411978.
 33. Tayler, M.C.D.; Levitt, M.H. Singlet Nuclear Magnetic Resonance of Nearly-Equivalent Spins. *Phys. Chem. Chem. Phys.* **2011**, *13*, 5556–5560, doi:10.1039/C0CP02293D.
 34. Nasibulov, E.A.; Pravdivtsev, A.N.; Yurkovskaya, A.V.; Lukzen, N.N.; Vieth, H.-M.; Ivanov, K.L. Analysis of Nutation Patterns in Fourier-Transform NMR of Non-Thermally Polarized Multispin Systems. *Z. Phys. Chem.* **2013**, *227*, 929–953, doi:10.1524/zpch.2013.0397.
 35. Barskiy, D.A.; Salnikov, O.G.; Shchepin, R.V.; Feldman, M.A.; Coffey, A.M.; Kovtunov, K.V.; Koptyug, I.V.; Chekmenev, E.Y. NMR SLIC Sensing of Hydrogenation Reactions Using Parahydrogen in Low Magnetic Fields. *J. Phys. Chem. C* **2016**, *120*, 29098–29106, doi:10.1021/acs.jpcc.6b07555.

-
36. Grohmann, T.; Leibscher, M. Nuclear Spin Selective Alignment of Ethylene and Analogues. *J. Chem. Phys.* **2011**, *134*, 204316, doi:10.1063/1.3595133.
37. Chapovsky, P.L.; Hermans, L.J.F. Nuclear Spin Conversion in Polyatomic Molecules. *Annu. Rev. Phys. Chem.* **1999**, *50*, 315–345, doi:10.1146/annurev.physchem.50.1.315.
38. Chapovsky, P.L.; Zhivonitko, V.V.; Koptuyug, I.V. Conversion of Nuclear Spin Isomers of Ethylene. *J. Phys. Chem. A* **2013**, *117*, 9673–9683, doi:10.1021/jp312322f.
39. San Fabián, J.; Casanueva, J.; Díez, E.; Esteban, A.L. Spin–Spin Coupling Constants in Ethylene: Equilibrium Values. *Chem. Phys. Lett.* **2002**, *361*, 159–168, doi:10.1016/S0009-2614(02)00949-1.
40. Kaski, J.; Lantto, P.; Vaara, J.; Jokisaari, J. Experimental and Theoretical Ab Initio Study of the ^{13}C – ^{13}C Spin–Spin Coupling and ^1H and ^{13}C Shielding Tensors in Ethane, Ethene, and Ethyne. *J. Am. Chem. Soc.* **1998**, *120*, 3993–4005, doi:10.1021/ja972936m.
41. Carrington, A.; McLachlan, A.D. *Introduction to Magnetic Resonance with Applications to Chemistry and Chemical Physics*; Harper & Row: New York, 1967;
42. DeVience, S.J.; Walsworth, R.L.; Rosen, M.S. Preparation of Nuclear Spin Singlet States Using Spin-Lock Induced Crossing. *Phys. Rev. Lett.* **2013**, *111*, 173002, doi:10.1103/PhysRevLett.111.173002.
43. Cavallari, E.; Carrera, C.; Boi, T.; Aime, S.; Reineri, F. Effects of Magnetic Field Cycle on the Polarization Transfer from Parahydrogen to Heteronuclei through Long-Range J-Couplings. *J. Phys. Chem. B* **2015**, *119*, 10035–10041, doi:10.1021/acs.jpcc.5b06222.
44. Schmidt, A.B.; Berner, S.; Schimpf, W.; Müller, C.; Lickert, T.; Schwaderlapp, N.; Knecht, S.; Skinner, J.G.; Dost, A.; Rovedo, P.; et al. Liquid-State Carbon-13 Hyperpolarization Generated in an MRI System for Fast Imaging. *Nat. Commun.* **2017**, *8*, ncomms14535, doi:10.1038/ncomms14535.
45. Cavallari, E.; Carrera, C.; Sorge, M.; Bonne, G.; Muchir, A.; Aime, S.; Reineri, F. The ^{13}C Hyperpolarized Pyruvate Generated by ParaHydrogen Detects the Response of the Heart to Altered Metabolism in Real Time. *Sci. Rep.* **2018**, *8*, 8366, doi:10.1038/s41598-018-26583-2.
46. Kovtunov, K.V.; Pokochueva, E.; Salnikov, O.; Cousin, S.; Kurzbach, D.; Vuichoud, B.; Jannin, S.; Chekmenev, E.; Goodson, B.; Barskiy, D.; et al. Hyperpolarized NMR: D-DNP, PHIP, and SABRE. *Chem. Asian J.* **2018**, *13*, 1857–1871, doi:10.1002/asia.201800551.
47. Lee, W.T.; Zheng, G.; Talbot, C.L.; Tong, X.; D’Adam, T.; Parnell, S.R.; Veer, M.D.; Jenkin, G.; Polglase, G.R.; Hooper, S.B.; et al. Hyperpolarised Gas Filling Station for Medical Imaging Using Polarised ^{129}Xe and ^3He . *Magn. Reson. Imag.* **2021**, doi:10.1016/j.mri.2021.02.010.
48. Reineri, F.; Viale, A.; Ellena, S.; Boi, T.; Daniele, V.; Gobetto, R.; Aime, S. Use of Labile Precursors for the Generation of Hyperpolarized Molecules from Hydrogenation with Parahydrogen and Aqueous-Phase Extraction. *Angew. Chem. Int. Ed.* **2011**, *50*, 7350–7353, doi:10.1002/anie.201101359.
49. Chukanov, N.V.; Salnikov, O.G.; Shchepin, R.V.; Kovtunov, K.V.; Koptuyug, I.V.; Chekmenev, E.Y. Synthesis of Unsaturated Precursors for Parahydrogen-Induced Polarization and Molecular Imaging of $1\text{-}^{13}\text{C}$ -Acetates and $1\text{-}^{13}\text{C}$ -Pyruvates via Side Arm Hydrogenation. *ACS Omega* **2018**, *3*, 6673–6682, doi:10.1021/acsomega.8b00983.
50. Nelson, S.J.; Kurhanewicz, J.; Vigneron, D.B.; Larson, P.E.Z.; Harzstark, A.L.; Ferrone, M.; Criekinge, M. van; Chang, J.W.; Bok, R.; Park, I.; et al. Metabolic Imaging of Patients with Prostate Cancer Using Hyperpolarized [$1\text{-}^{13}\text{C}$]Pyruvate. *Sci. Transl. Med.* **2013**, *5*, 198ra108–198ra108, doi:10.1126/scitranslmed.3006070.
51. Cunningham, C.H.; Lau, J.Y.C.; Chen, A.P.; Geraghty, B.J.; Perks, W.J.; Roifman, I.; Wright, G.A.; Connelly, K.A. Hyperpolarized ^{13}C Metabolic MRI of the Human Heart. *Circ. Res.* **2016**, *119*, 1177–1182.

-
52. Berner, S.; Schmidt, A.B.; Zimmermann, M.; Pravdivtsev, A.N.; Glöggler, S.; Hennig, J.; von Elverfeldt, D.; Hövener, J.-B. SAMBADENA Hyperpolarization of ^{13}C -Succinate in an MRI: Singlet-Triplet Mixing Causes Polarization Loss. *ChemistryOpen* **2019**, *8*, 728–736, doi:10.1002/open.201900139.
 53. Schmidt, A.B.; Brahms, A.; Ellermann, F.; Knecht, S.; Berner, S.; Hennig, J.; Elverfeldt, D. von; Herges, R.; Hövener, J.-B.; Pravdivtsev, A. Selective Excitation of Hydrogen Doubles the Yield and Improves the Robustness of Parahydrogen-Induced Polarization of Low- γ Nuclei. *Phys. Chem. Chem. Phys.* **2021**, doi:10.1039/D1CP04153C.
 54. Olsson, L.E.; Chai, C.-M.; Axelsson, O.; Karlsson, M.; Golman, K.; Petersson, J.S. MR Coronary Angiography in Pigs with Intraarterial Injections of a Hyperpolarized ^{13}C Substance. *Magn. Reson. Med.* **2006**, *55*, 731–737, doi:10.1002/mrm.20847.
 55. Pravdivtsev, A.; Brahms, A.; Kienitz, S.; Sönnichsen, F.D.; Hövener, J.-B.; Herges, R. Catalytic Hydrogenation of Trivinyl Orthoacetate: Mechanisms Elucidated by Parahydrogen Induced Polarization. *ChemPhysChem* **2020**, cphc.202000957, doi:10.1002/cphc.202000957.
 56. Pravdivtsev, A.N.; Yurkovskaya, A.V.; Lukzen, N.N.; Ivanov, K.L.; Vieth, H.-M. Highly Efficient Polarization of Spin-1/2 Insensitive NMR Nuclei by Adiabatic Passage through Level Anticrossings. *J. Phys. Chem. Lett.* **2014**, *5*, 3421–3426, doi:10.1021/jz501754j.
 57. Knecht, S.; Blanchard, J.W.; Barskiy, D.; Cavallari, E.; Dagys, L.; Dyke, E.V.; Tsukanov, M.; Bliemel, B.; Münnemann, K.; Aime, S.; et al. Rapid Hyperpolarization and Purification of the Metabolite Fumarate in Aqueous Solution. *PNAS* **2021**, *118*, doi:10.1073/pnas.2025383118.
 58. Eills, J.; Cavallari, E.; Kircher, R.; Matteo, G.D.; Carrera, C.; Dagys, L.; Levitt, M.H.; Ivanov, K.L.; Aime, S.; Reineri, F.; et al. Singlet-Contrast Magnetic Resonance Imaging: Unlocking Hyperpolarization with Metabolism**. *Angew. Chem. Int. Ed.* **2021**, *60*, 6791–6798, doi:https://doi.org/10.1002/anie.202014933.
 59. Franzoni, M.B.; Buljubasich, L.; Spiess, H.W.; Münnemann, K. Long-Lived ^1H Singlet Spin States Originating from Para-Hydrogen in Cs-Symmetric Molecules Stored for Minutes in High Magnetic Fields. *J. Am. Chem. Soc.* **2012**, *134*, 10393–10396, doi:10.1021/ja304285s.
 60. Pravdivtsev, A.N.; Hövener, J.-B. Simulating Non-Linear Chemical and Physical (CAP) Dynamics of Signal Amplification By Reversible Exchange (SABRE). *Chem. Eur. J.* **2019**, *25*, 7659–7668, doi:10.1002/chem.201806133.
 61. Rodríguez-Carvajal, J.; Bourée, F. Symmetry and Magnetic Structures. *EPJ Web Conf.* **2012**, *22*, 00010, doi:10.1051/epjconf/20122200010.